TABLE 2. Summary of outcome

Complications		
Infections	Possible invasive pulmonary aspergillosis	1
	Cytomegalovirus reactivation	10
	Cytomegalovirus retinitis	2
	Adenovirus hemorrhagic cystitis	2
Acute GVHD	0	6
	I	4
	II	1
	III	1
	IV	0
Chronic GVHD	None	6
	Limited	2
	Extensive	0
	Not evaluable	4
Outcome		
Status before transplantation	Current status	
Remission 4	Alive in remission	3
	Died in remission	1 (radiation pneumonitis)
Active disease 8	Alive in remission	2
	Alive after relapse	2
	Died after relapse	3
	Died in remission	1 (thrombotic microangiopathy)

GVHD, graft-versus-host disease.

stitution after transplantation was evaluated in greater detail by the quantification of CD3+/CD4+, CD3+/CD8+, CD3−/CD19+, and CD3−/CD56+ cells, and compared with that after transplantation from an HLA-identical sibling donor or a matched unrelated donor (Fig. 4). The numbers of CD3+/CD4+ and CD3+/CD8+ cells were significantly lower than those after transplantation from an HLA-identical sibling donor or a matched unrelated donor during the first 2 months after transplantation. However, the numbers of CD3+/CD4+ and CD3+/CD8+ cells caught up with those after matched unrelated transplantation on day 90. CD3−/CD56+ and CD3−/CD19+ cells recovered earlier than T cells.

CMV-specific T-cell recovery was evaluated by tetramer assay in six patients who had HLA-A*0201 or HLA-A*2402. CMV-specific cytotoxic T lymphocytes were detected on day 90 after transplantation in two patients, at 0.03% and 0.25% of CD8+ T cells, respectively. Both patients had CMV reactivation before the detection of CMV-specific cytotoxic T lymphocytes. As a functional assay, a PHA stimulation test was performed using peripheral lymphocytes in three patients on days 120, 377, and 509, respectively, after transplantation. The stimulation index was 415.2 and 391.0, respectively, in the two patients who were tested more than 1 year after transplantation. Considering that the 95% confidence interval for the stimulation index in the normal population is 74 and 508, peripheral T cells in these patients have a normal proliferative response to PHA stimulation. Although the stimulation index was only 10.7 in the patient who was tested on day 120, at that time only 6% of the peripheral lymphocytes were T cells, and thus the response was within the normal range when corrected for the percentage of T cells.

DISCUSSION

We evaluated the safety of haploidentical peripheral blood stem-cell transplantation from a two or three loci-mismatched family member using in vivo alemtuzumab. There was no graft rejection, and the incidence of grades III to IV acute GVHD was only 9%, almost equivalent to that after transplantation from an HLA-matched sibling donor (*3*). The median age of the 12 patients was 49.5 years, and 9 and 6 patients were older than 40 and 50 years, respectively. Thus, the patients in this study were much older than those in previous reports on haploidentical stem-cell transplantation (*5*, *25*, *26*). Nevertheless, nonrelapse mortality was observed in only two patients.

A major concern with this strategy was infectious complications caused by prolonged immunosuppression. In fact, CD3+/CD4+ and CD3+/CD8+ T cells were strongly suppressed within 2 months after transplantation, which was reflected by the high incidence of CMV reactivation. However, this did not translate into the development of severe infections. None of the patients died of infectious causes. Another concern was relapse after transplantation. Five of the eight patients who underwent transplantation for active disease had a relapse, whereas this was not seen in any of the three patients who underwent transplantation in first remission. Therefore, the dose of alemtuzumab is appropriate for patients with early disease, whereas it may be better to reduce

the dose of alemtuzumab for patients with active disease, considering the low incidence of severe GVHD in this study.

The transplantation procedure was simplified and the cost was reduced by the omission of ex vivo graft manipulation. Antithymocyte globulin (ATG) could also be used for in vivo T-cell depletion. However, considering the results of HLA-matched transplantation, the prophylactic effect of alemtuzumab against GVHD seemed to be much stronger than that of ATG (*14, 15, 20, 27*). The unique pharmacokinetic profile, in which a lympholytic concentration remains for approximately 2 months after transplantation, may contribute to the potent effect against GVHD (*13*). Depletion of host dendritic cells, which also express CD52, could be another mechanism to prevent GVHD, because host antigen-presenting cells have been shown to be important for the development of GVHD in mouse models (*28*). Alemtuzumab may be more appropriate for clinical use than ATG, because alemtuzumab is a recombinant monoclonal antibody with a consistent quality, whereas lot-to-lot variability of ATG cannot be avoided, because ATG is prepared by immunizing horses or rabbits with human lymphoid cells. Another advantage of alemtuzumab is that it kills not only T cells but also B cells, and thus there may be a lower risk of posttransplant lymphoproliferative disorders. A possible disadvantage of alemtuzumab is that alemtuzumab may kill NK cells, which may be important for a graft-versus-leukemia/lymphoma effect (*29*). However, the recovery of NK cells was observed early after transplantation in this study and was equivalent to that after matched unrelated donor transplantation. As further evidence that the lympholytic effect of alemtuzumab on NK cells is weaker than that on T cells, alemtuzumab "in the bag" resulted in the 99.8% and 94% depletion of CD4+ and CD8+ T cells, respectively, whereas 30% of NK cells were conserved in the graft (*30*).

CONCLUSION

Unmanipulated hematopoietic stem-cell transplantation was safely performed from a two or three loci-mismatched family member using in vivo alemtuzumab. This novel therapeutic approach could be applied to patients aged more than 50 years without the need for an HLA-matched donor or any specific devices. [AU: Please cite Table 2 in text.]

REFERENCES

1. Anasetti C. Hematopoietic cell transplantation from HLA partially matched donors. In: Thomas ED, Blume KG, Forman SJ, eds. Hematopoietic cell transplantation. Malden, Blackwell Science 1999, p 904.
2. Beatty P, Henslee-Downey PJ. HLA-mismatched family member hematopoietic stem cell transplantation. In: Atkinson K, ed. Clinical bone marrow and blood stem cell transplantation. Cambridge, Cambridge University Press 2000, p 603.
3. Kanda Y, Chiba S, Hirai H, et al. Allogeneic hematopoietic stem cell transplantation from family members other than HLA-identical siblings over the last decade (1991–2000). *Blood* 2003; 102: 1541.
4. Anasetti C, Amos D, Beatty PG, et al. Effect of HLA compatibility on engraftment of bone marrow transplants in patients with leukemia or lymphoma. *N Engl J Med* 1989; 320: 197.
5. Aversa F, Tabilio A, Velardi A, et al. Treatment of high-risk acute leukemia with T-cell-depleted stem cells from related donors with one fully mismatched HLA haplotype. *N Engl J Med* 1998; 339: 1186.
6. Hale G. The CD52 antigen and development of the CAMPATH antibodies. *Cytotherapy* 2001; 3: 137.
7. Hale G, Slavin S, Goldman JM, et al. Alemtuzumab (Campath-1H) for treatment of lymphoid malignancies in the age of nonmyeloablative conditioning? *Bone Marrow Transplant* 2002; 30: 797.
8. Hale G, Cobbold S, Waldmann H. T cell depletion with CAMPATH-1 in allogeneic bone marrow transplantation. *Transplantation* 1988; 45: 753.
9. Hale G, Zhang MJ, Bunjes D, et al. Improving the outcome of bone marrow transplantation by using CD52 monoclonal antibodies to prevent graft-versus-host disease and graft rejection. *Blood* 1998; 92: 4581.
10. Slavin S, Or R, Weiss L, et al. Elimination of graft versus host disease in matched allogeneic leukemic transplant recipients using CAMPATH-1. *Adv Exp Med Biol* 1985; 186: 813.
11. Riechmann L, Clark M, Waldmann H, et al. Reshaping human antibodies for therapy. *Nature* 1988; 332: 323.
12. Rebello P, Cwynarski K, Varughese M, et al. Pharmacokinetics of CAMPATH-1H in BMT patients. *Cytotherapy* 2001; 3: 261.
13. Morris EC, Rebello P, Thomson KJ, et al. Pharmacokinetics of alemtuzumab used for in vivo and in vitro T-cell depletion in allogeneic transplantations: relevance for early adoptive immunotherapy and infectious complications. *Blood* 2003; 102: 404.
14. Chakraverty R, Peggs K, Chopra R, et al. Limiting transplantation-related mortality following unrelated donor stem cell transplantation by using a nonmyeloablative conditioning regimen. *Blood* 2002; 99: 1071.
15. Kottaridis PD, Milligan DW, Chopra R, et al. In vivo CAMPATH-1H prevents graft-versus-host disease following nonmyeloablative stem cell transplantation. *Blood* 2000; 96: 2419.
16. Vassiliou GS, Webb DK, Pamphilon D, et al. Improved outcome of alternative donor bone marrow transplantation in children with severe aplastic anaemia using a conditioning regimen containing low-dose total body irradiation, cyclophosphamide and Campath. *Br J Haematol* 2001; 114: 701.
17. Kanda Y, Mineishi S, Saito T, et al. Long-term low-dose acyclovir against varicella-zoster virus reactivation after allogeneic hematopoietic stem cell transplantation. *Bone Marrow Transplant* 2001; 28: 689.
18. Kanda Y, Mineishi S, Saito T, et al. Response-oriented preemptive therapy against cytomegalovirus disease with low-dose ganciclovir: a prospective evaluation. *Transplantation* 2002; 73: 568.
19. Przepiorka D, Weisdorf D, Martin P, et al. 1994 Consensus Conference on Acute GVHD Grading. *Bone Marrow Transplant* 1995; 15: 825.
20. Saito T, Kanda Y, Kami M, et al. Therapeutic potential of a reduced-intensity preparative regimen for allogeneic transplantation with cladribine, busulfan, and antithymocyte globulin against advanced/refractory acute leukemia/lymphoma. *Clin Cancer Res* 2002; 8: 1014.
21. Kuzushima K, Hayashi N, Kimura H, et al. Efficient identification of HLA-A*2402-restricted cytomegalovirus-specific CD8(+) T-cell epitopes by a computer algorithm and an enzyme-linked immunospot assay. *Blood* 2001; 98: 1872.
22. Cwynarski K, Ainsworth J, Cobbold M, et al. Direct visualization of cytomegalovirus-specific T-cell reconstitution after allogeneic stem cell transplantation. *Blood* 2001; 97: 1232.
23. Saito T, Kanda Y, Nakai K, et al. Immune reconstitution following reduced-intensity transplantation with cladribine, busulfan, and antithymocyte globulin: serial comparison with conventional myeloablative transplantation. *Bone Marrow Transplant* 2003; 32: 601.
24. Simon R. Optimal two-stage designs for phase II clinical trials. *Control Clin Trials* 1989; 10: 1.
25. Kato S, Yabe H, Yasui M, et al. Allogeneic hematopoietic transplantation of CD34+ selected cells from an HLA haplo-identical related donor. A long-term follow-up of 135 patients and a comparison of stem cell source between the bone marrow and the peripheral blood. *Bone Marrow Transplant* 2000; 26: 1281.
26. Yamasaki S, Ohno Y, Taniguchi S, et al. Allogeneic peripheral blood stem cell transplantation from two- or three-loci-mismatched related donors in adult Japanese patients with high-risk hematologic malignancies. *Bone Marrow Transplant* 2004; 33: 279.
27. Slavin S, Nagler A, Naparstek E, et al. Nonmyeloablative stem cell transplantation and cell therapy as an alternative to conventional bone marrow transplantation with lethal cytoreduction for the treatment of malignant and nonmalignant hematologic diseases. *Blood* 1998; 91: 756.
28. Shlomchik WD, Couzens MS, Tang CB, et al. Prevention of graft versus host disease by inactivation of host antigen-presenting cells. *Science* 1999; 285: 412.
29. Ruggeri L, Capanni M, Urbani E, et al. Effectiveness of donor natural killer cell alloreactivity in mismatched hematopoietic transplants. *Science* 2002; 295: 2097.
30. Koh LP, Rizzieri DA, Long GD, et al. Campath-1H, T-cell depleted nonmyeloablative peripheral blood stem cell transplantation from 3–6/6 HLA matched family members. *Blood* 2002; 100(suppl 1): 638a.

Graft-versus-Tumor Effect Against Advanced Pancreatic Cancer after Allogeneic Reduced-Intensity Stem Cell Transplantation

Yoshinobu Kanda,[1,5] Yutaka Komatsu,[2] Masaaki Akahane,[3] Shigeyuki Kojima,[4] Yuki Asano-Mori,[1] Minoru Tada,[2] Kumi Oshima,[1] Hiroyuki Isayama,[2] Seishi Ogawa,[1] Toru Motokura,[1] Shigeru Chiba,[1] Kuni Ohtomo,[3] Masao Omata,[2] and Hisamaru Hirai[1]

Background. The prognosis of advanced pancreatic cancer is extremely poor and therefore a novel treatment strategy is desired. The authors thus started a prospective study of allogeneic reduced-intensity hematopoietic stem cell transplantation (RIST) for patients with advanced pancreatic cancer to evaluate the feasibility and efficacy of this approach for such patients.

Methods. Only patients with pathologically proven pancreatic cancer that was locally advanced or metastatic and not amenable to curative resection were included. The conditioning regimen consisted of gemcitabine, fludarabine, and busulfan.

Results. In the first stage of this study, the authors treated seven patients. Treatment-related mortality before day 100 was observed in one patient. The median survival after RIST was 229 days. An objective response on computed tomographic scan was observed in two patients and another had a tumor marker response. Marked tumor shrinkage was observed in one of the remaining patients after donor lymphocyte infusion. These antitumor effects appeared after the effect of the conditioning regimen had disappeared. In addition, some of these responses were associated with an increase in the serum anticarcinoembryonic antigen antibody level.

Conclusions. Pancreatic cancer appeared to be sensitive to a graft-versus-tumor effect; therefore, a larger clinical study with a refined strategy is warranted.

Keywords: Reduced-intensity stem cell transplantation, Minitransplantation, Pancreatic cancer, Graft-versus-tumor effect, Graft-versus-host disease.

(*Transplantation* 2005;79: 821–827)

Pancreatic cancer is the fifth most common cause of cancer-related mortality in Japan and the United States. The median duration of survival in advanced pancreatic cancer is less than 6 months, even when treated with gemcitabine (*1*), and therefore a novel treatment strategy is desired. Allogeneic nonmyeloablative or reduced-intensity hematopoietic stem cell transplantation (RIST) is a recently developed treatment approach for obtaining a graft-versus-tumor (GVT) effect without the toxicity associated with a myeloablative conditioning regimen (*2–6*). This treatment strategy is suitable for patients with solid tumors, because patients with advanced solid tumors are generally clinically infirm, and also a strong antitumor effect cannot be expected with an intensification of chemotherapy. In addition, a GVT effect has been noted in several solid tumors after conventional hematopoietic stem-cell transplantation (*7, 8*). Based on this background, RIST has been investigated for use against solid cancers since the late 1990s and its feasibility has already been demonstrated in several studies (*9–14*). However, there is still little information available regarding its efficacy against individual solid cancers. Childs et al. showed an excellent response rate of 53% after RIST against metastatic renal cell cancer (*9*). A GVT effect against renal cell cancer was confirmed in trials by other centers. In contrast, RIST against metastatic melanoma, which has been considered to be a good candidate for immunotherapy, resulted in a miserable outcome (*15*). Therefore, it is difficult to predict whether a GVT effect can be achieved against an individual tumor. We started a prospective study to evaluate the feasibility and efficacy of RIST against advanced pancreatic cancer after ethical approval in April 2002.

PATIENTS AND METHODS

Patients

Eligible patients were younger than 70 years of age and had pathologically proven pancreatic adenocarcinoma, which was locally advanced or metastatic and not amenable to curative resection. Patients had a human leukocyte antigen (HLA)-matched sibling or a family donor with a single mismatched HLA antigen. Patients with a poor performance status (Eastern Cooperative Oncology Group 2–4) and those with severely impaired organ function were excluded. Patients and donors gave their written informed consent to participate in this study.

Twelve patients with pancreatic cancer fulfilled the inclusion criteria but lacked a suitable donor. They were considered control patients. Four of them had metastatic lesions, whereas eight had locally advanced disease. Nine received

[1] Department of Cell Therapy & Transplantation Medicine, University of Tokyo, Tokyo, Japan.
[2] Department of Gastroenterology, University of Tokyo, Tokyo, Japan.
[3] Department of Radiology, University of Tokyo, Tokyo, Japan.
[4] R & D Center, BML, Inc., Kawagoe, Japan.
[5] Address correspondence to: Yoshinobu Kanda, M.D., Department of Cell Therapy & Transplantation Medicine, University of Tokyo, 7-3-1 Hongo, Bunkyo-ku, Tokyo 113-8655, Japan. E-mail: ycanda-tky@umin.ac.jp.
Received 28 September 2004. Revision requested 27 October 2004. Accepted 10 November 2004.

ISSN 0041-1337/05/7907-821
DOI: 10.1097/01.TP.0000153507.94980.A5

chemotherapy with gemcitabine, whereas three were observed without chemotherapy.

Transplantation Procedure

Donors received granulocyte colony-stimulating factor at 200 $\mu g/m^2$ administered subcutaneously twice daily starting 3 days before the first collection of peripheral blood stem cells until the end of collection. Leukapheresis was performed daily until more than 2.0×10^6 $CD34^+$ cells/kg of the recipient's body weight were collected. Collected cells were then cryopreserved using standard techniques without ex vivo manipulation.

The conditioning regimen consisted of gemcitabine (1,000 mg/m^2/day as a 90-min infusion on days −16, −9, and −2) (*16*), fludarabine (30 mg/m^2/day as a 30-min infusion on days −8 to −3), and busulfan (4 mg/kg/day administered orally in four divided doses on days −6 and −5) (*4, 17*). Graft-versus-host disease (GVHD) prophylaxis was performed with cyclosporine (CsA) (3 mg/kg/day as a continuous infusion) and short-term methotrexate (10 mg/m^2 on day 1 and 7 mg/m^2 on days 3 and 6). Frozen peripheral blood stem cells were thawed and infused on day 0. CsA was decreased at 10% per week from day 30 and discontinued by day 100 unless the patient developed acute GVHD. In patients with progressive disease without any evidence of acute GVHD, CsA was rapidly tapered over a 4-week period. Acute GVHD was graded as previously described (*18*). Grade II to IV acute GVHD was treated with methylprednisolone at 1 mg/kg per day, except for grade II GVHD limited to the skin, which was treated with topical steroid ointment.

Prophylaxis against bacterial, fungal, and *Pneumocystis carinii* infection consisted of tosufloxacin, fluconazole, and sulfamethoxazole-trimethoprim. As prophylaxis against herpes simplex virus infection, acyclovir was administered at 500 mg per day intravenously or 1,000 mg per day orally from days −7 to 35, followed by long-term low-dose (200 mg/day) oral administration (*19*). Patients received granulocyte colony-stimulating factor (filgrastim) at 300 μg per day by 3-hr infusion beginning on day 7 until the neutrophil count recovered to $500/mm^3$. Cytomegalovirus antigenemia assay using C10/C11 antibody was performed at least once per week after engraftment. Ganciclovir was started when more than two positive cells were detected on two slides (*20, 21*).

Donor lymphocyte infusion (DLI) was performed for patients who had progressive disease and did not develop GVHD even after CsA was discontinued. The initial $CD3^+$ cell dose was 1 to 3×10^7 cells/kg and the dose was escalated every 4 weeks when the patient did not develop tumor response or GVHD.

Chimerism and Immunologic Analyses

Host-donor cell chimerism after transplantation was analyzed monthly by sex-chromosome fluorescent in situ hybridization or the short tandem repeat method after transplantation (*22*). The serum anti-carcinoembryonic antigen (CEA) antibody level was determined by enzyme-linked immunosorbent assay as previously described (*23*). Briefly, 96-well microplates were coated overnight at 4°C with a 5-μg/mL CEA preparation. The plates were washed and blocked for 2 hr at room temperature with 200 μL/well of a 0.1% Tween20, 5% nonfat dry milk, phosphate-buffered saline solution to prevent nonspecific binding. After the plates were washed further, 50 μL of 1:100 diluted patient sera was added per well and incubated for 2 hr at room temperature. After the plates were washed five times, 50 μL of horseradish peroxidase-labeled anti-human immunoglobulin G antiserum at 0.1 μg/mL in blocking buffer was added per well. The plates were incubated for 90 min at room temperature and then washed five times. The conjugated anti-CEA antibody was detected by adding 100 μL of tetramethylbenzidine substrate per well, incubating for 30 min at room temperature, adding 50 μL of 2N H_2SO_4 per well to terminate the reaction, and measuring the absorbance at 450 nm. The net anti-CEA antibody absorbance was determined by subtracting the absorbance of a noncoated well from the gross absorbance.

Outcome Measures

The primary endpoint of this study was transplant-related mortality within 100 days after transplantation. The secondary endpoint was the tumor response within 6 months after transplantation. Toxicities associated with the conditioning regimen were graded according to the criteria of Bearman et al. (*24*). Objective tumor response was evaluated by an independent radiologist using a monthly computed tomographic (CT) scan. Complete response was defined as disappearance of all clinical evidence of tumor for a minimum of 4 weeks. Minor and partial responses were defined as decreases of 25% to 50% and greater than 50%, respectively, in the sum of the products of the maximum diameter and its perpendicular diameter of all measurable lesions for a minimum of 4 weeks (*1*). The tumor marker response was evaluated by biweekly measurement of the serum CA19-9 level, because imaging modalities including ultrasonography and CT scan are

TABLE 1. Characteristics of the patients

Patient	Age/sex	Prior treatment	Duration from Dx to transplant (mo)	Meta	HLA	No. of $CD34^+$ cells
1	48/M	Gem	3	—	6/6	4.8×10^6/kg
2	40/M	Gem+RT, Gem	9	—	6/6	5.1×10^6/kg
3	57/F	Gem+CDDP	4	Liver	6/6	4.0×10^6/kg
4	36/F	Gem	3	Liver	6/6	2.9×10^6/kg
5	59/M	Gem	2	—	6/6	5.6×10^6/kg
6	66/F	Gem	2	Peritonitis	6/6	2.0×10^6/kg
7	61/M	Gem+RT	12	Liver	6/6	3.0×10^6/kg

Dx, diagnosis; Meta, metastatic lesion; Gem, gemcitabine; RT, local radiation; CDDP, cisplatin.

TABLE 2. Outcome after RIST

Patient	Donor chimerism (%)	aGVHD	Objective response	Final outcome
1	100	III	MR	Died as a result of bacteremia on day 192
2	100	II	SD	Died as a result of PD on day 293
3	100	II[a]	MR[d]	Died as a result of PD on day 262
4	100	II[a]	PD	Died as a result of PD on day 72
5	100	II	SD[c,d]	Died as a result of PD on day 587
6	100	III[b]	PD	Died as a result of PD on day 229
7	100	III[a]	SD	Died as a result of pneumonia on day 83

[a] GVHD that occurred after the rapid tapering of immunosuppressants.
[b] GVHD that occurred after DLI.
[c] Partial response on tumor marker evaluation.
[d] Morphine was discontinued.
aGVHD, acute graft-versus-host disease; MR, minor response; SD, stable disease; PD, progressive disease; DLI, donor lymphocyte infusion.

not sufficient to determine the accurate tumor size of pancreatic cancer (*25*). For patients with a normal value of CA19-9 before RIST, CEA, Dupan-II, or Span-I was measured instead. A complete marker response was defined as normalization of the tumor marker for a minimum of 4 weeks. Minor and partial responses were defined as decreases of 25% to 50% and greater than 50%, respectively, in the tumor marker for a minimum of 4 weeks.

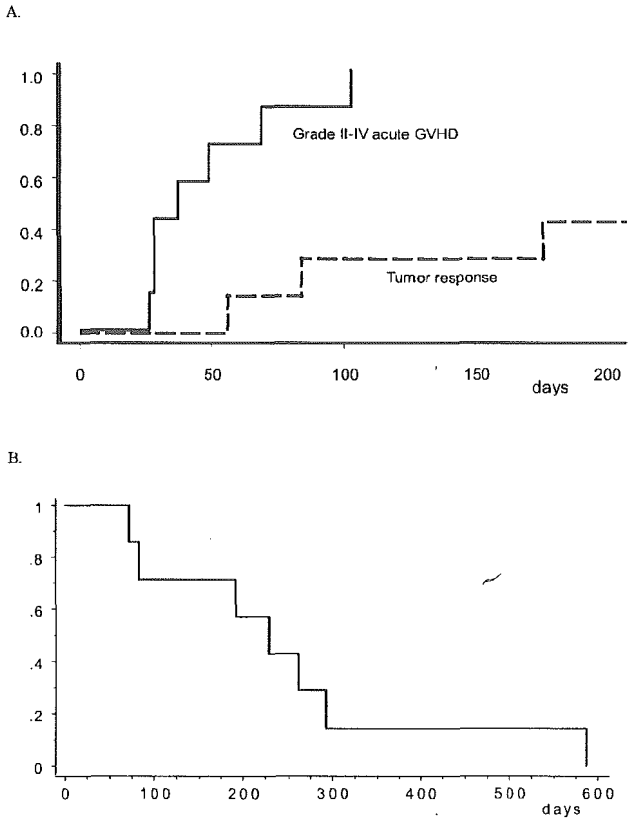

FIGURE 1. (A) Cumulative incidence of grade II to IV acute GVHD (*solid line*) and tumor response including both the objective response and the tumor marker response (*broken line*). (B) Overall survival after RIST against advanced pancreatic cancer.

Statistical Considerations

We defined success as the absence of early transplant-related mortality and planned seven and nine patients in the first and second stages of the study, with target and lower success rates of 80% and 50% and α and β errors of 10% and 10%, respectively (*26*). This is an analysis of the seven patients in the first stage. The cumulative incidence of tumor response was calculated by Gray's method considering death without response as a competing risk (*27*).

RESULTS

Patients

In the first stage of this study, seven patients with a median age of 57 years (range, 36–66 years) underwent RIST (Table 1). The duration from diagnosis to transplantation was 2 to 12 months. Four had metastatic disease and three had locally advanced disease. Prior treatment consisted of chemotherapy mainly with gemcitabine without an objective response, except for one patient (patient 2) who achieved a transient partial response after gemcitabine combined with local irradiation. All of the patients had progressive disease just before the conditioning regimen. All received a peripheral blood stem-cell graft from an HLA-identical sibling donor. The median number of $CD34^+$ cells in the graft was 4.0×10^6 cells/kg recipient body weight (range, 2.0–5.6 cells/kg). Three patients (patients 2, 5, and 6) underwent DLI for tumor progression 221, 336, and 69 days after transplantation, respectively. The dose of infused $CD3^+$ cells ranged between 2.7×10^7 and 1.8×10^8 cells/kg.

Regimen-Related Toxicity, Engraftment, and GVHD

Regimen-related toxicities were generally mild and well tolerated. Grade II to IV toxicity according to Bearman's grade was observed in two patients. One developed mild hepatic veno-occlusive disease, which recovered spontaneously. Another developed ileus caused by the pancreatic head tumor during the neutropenic period, which required nasogastric suction.

The median number of infused $CD34^+$ cells was 4.0×10^6 cells/kg (range, $2.0–5.6\times10^6$ cells/kg). Neutrophil engraftment was obtained within 12 days (range, 11–12 days)

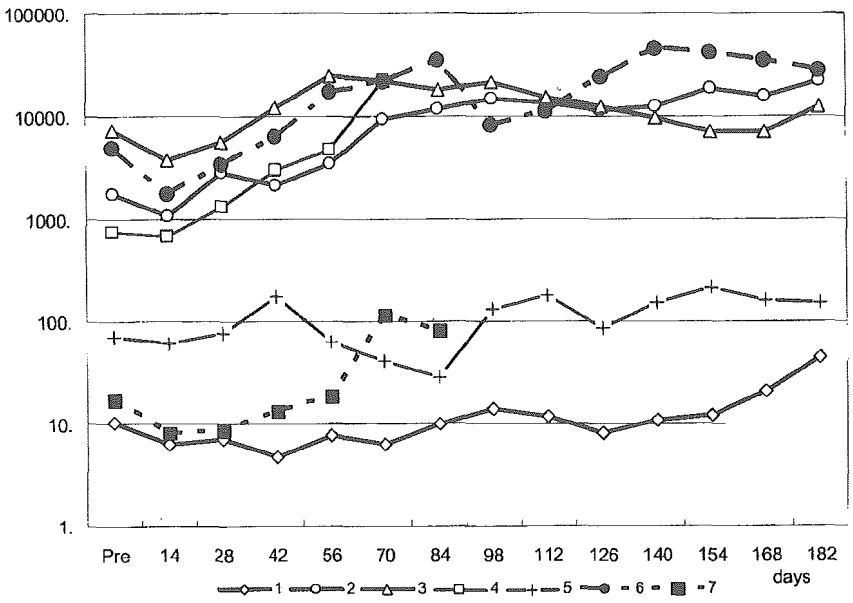

FIGURE 2. Serial changes in the values of tumor markers. CA19-9 was used all except patients 1 and 7, in whom CEA was measured instead because the CA19-9 level was within normal limits before transplantation. The units for the y-axis are units per milliliter for CA19-9 and nanograms per milliliter for CEA. A log scale was used for the y-axis to show serial data of all patients in one figure. Pre, pretransplant level.

after transplantation. Complete donor chimerism (>95%) was achieved in all patients by day 28 and maintained thereafter (Table 2). Grade II to III acute GVHD was observed in three patients (patients 1, 2, and 5) without rapid tapering of CsA, in three (patients 3, 4, and 7) after rapid tapering of CsA, and in one after DLI (Fig. 1A). Acute GVHD limited to the skin was cured with topical steroid only, whereas gut GVHD was successfully treated with systemic steroid.

Transplant-Related Mortality and Survival

Transplant-related mortality within 100 days after transplantation was observed in 1 patient (patient 7), who died as a result of pneumonia on day 83. Another patient (patient 1) died with bacteremia on day 192 caused by bacterial cholangitis. The other five patients died as a result of progressive disease. Median survival after RIST was 229 days (Fig. 1B), which was longer than the median survival of control patients after they were referred to our hospital (125 days), but this difference was not statistically significant.

Tumor Response

An objective minor response on CT scan was seen in two patients (patients 1 and 3) (Table 2 and Fig. 1A). Another patient (patient 5) achieved a partial tumor marker response. Two (patients 3 and 5) of the responders became free from all analgesics after achieving tumor regression.

As shown in Figure 2, the serum CA19-9 or CEA level generally increased within 6 to 8 weeks after transplantation after a transient decline associated with the conditioning chemotherapy. However, it stabilized (n=1) or began to decrease (n=3) thereafter, associated with the discontinuation of CsA or the development of GVHD. This suggests that the antitumor effect was caused by a GVT effect, not a chemotherapy effect. In particular, the serum CA19-9 level decreased from 25,180 U/mL on day 56 to 7,100 U/mL on day 154, with a tumor shrinkage on CT scan in patient 3 after the development of gut GVHD on day 69 (Fig. 3A). Evidence of a GVT effect against pancreatic cancer was also clearly seen in patient 6, who underwent DLI on day 69 for a progressive peritoneal metastatic lesion. The serum CA19-9 level decreased from 35,160 U/mL to 8,140 U/mL in 1 month, with an improvement of the peritoneal lesion on abdominal CT scan (Fig. 3B). However, these tumor responses were not durable and the response duration was between 28 and 98 days.

Serum Anti-CEA Antibody Level

Serum anti-CEA antibody levels were sequentially measured before and after RIST. The serum anti-CEA antibody level before RIST was higher than that in a normal population (n=3), with borderline significance (optical density, 0.109 ± 0.065 vs. 0.028 ± 0.030; $P=0.076$). It generally decreased 1 month after RIST with conditioning chemotherapy. Thereafter, an increase in the serum anti-CEA antibody level was observed in three patients. All three of these patients showed a tumor response, including one after DLI, whereas only one of the four patients without an increase in the serum anti-CEA antibody level showed a response. As shown in Figure 4, the increase in the serum anti-CEA antibody level was simultaneously associated with, or followed by, a decrease in the tumor marker level. However, this response was suppressed by the administration of high-dose steroid (Fig. 4A).

The increase in the serum anti-CEA level did not reflect nonspecific immune recovery, because we did not observe a significant relationship between serum anti-CEA antibody levels and antibody levels against other viral antigens (data not shown). In addition, the increase in the serum anti-CEA level did not result from a decrease in the serum CEA antigen that may absorb anti-CEA antibody, because we did not observe a negative relationship between them (data not shown).

DISCUSSION

In this study, we showed that RIST is a feasible treatment for patients with advanced pancreatic cancer. In addition, an objective response and a tumor marker response were observed in two and one of seven patients, respectively, who

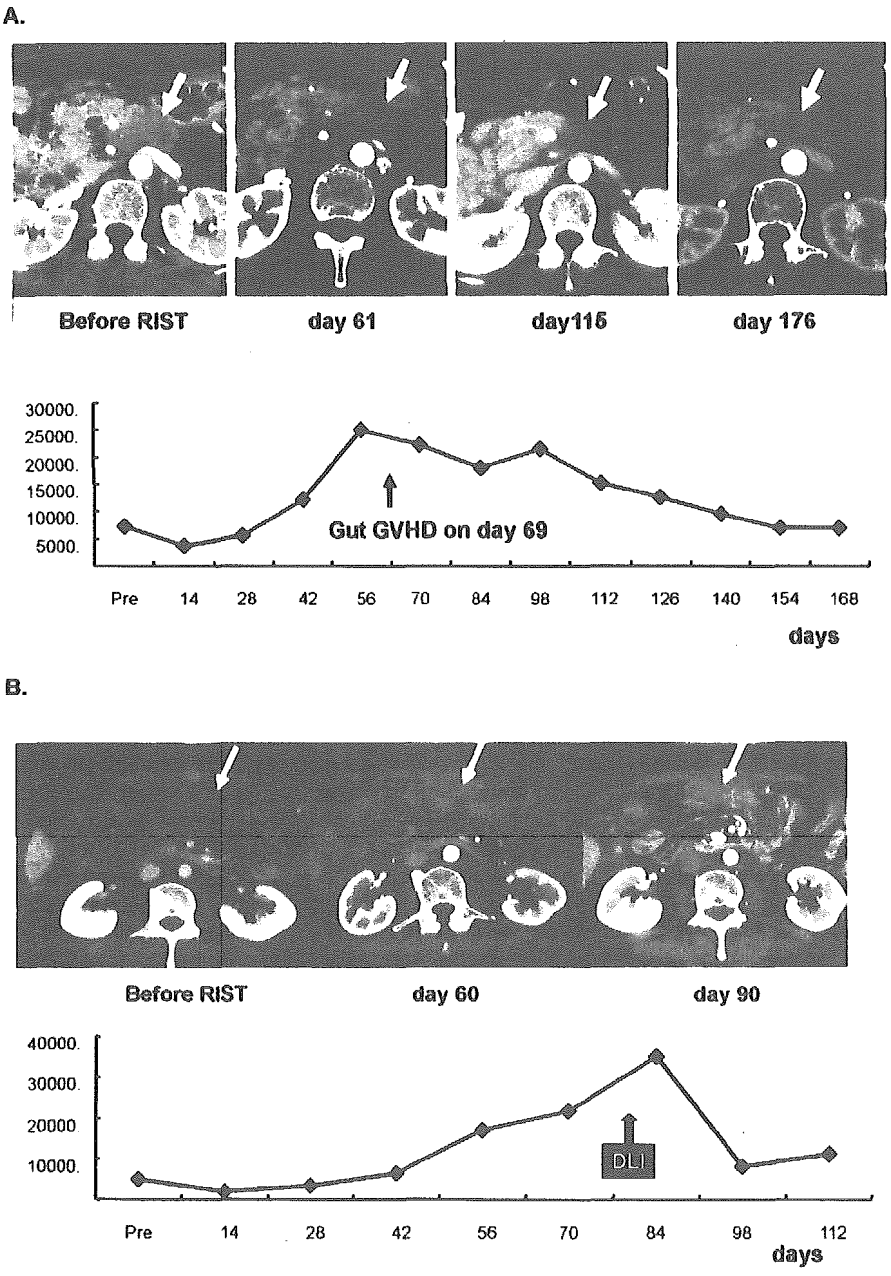

FIGURE 3. (A) Serial abdominal CT scans and serum CA19-9 levels of a patient (patient 3) who achieved an objective response after transplantation. The pancreatic body tumor shrunk and the serum CA19-9 level decreased after the development of gut GVHD. (B) Serial abdominal CT scans and serum CA19-9 levels of a patient (patient 6) who achieved an objective response after DLI. The peritoneal lesion worsened in the first 2 months after transplantation. However, the tumor began to shrink and the serum CA19-9 level rapidly decreased after DLI.

had not responded to conventional treatments. A response to DLI was seen in another patient. Although it is too early to evaluate survival after RIST, the median survival of 229 days might be better than that after conventional treatments. However, the tumor response was not durable, and all of the responding patients eventually died as a result of tumor progression.

It has been shown that at least 2 months are required to obtain a GVT effect after RIST against solid cancers. Childs et al. reported that tumor growth was frequently observed during the first few months after RIST for renal cell cancer (*9*). Therefore, we added gemcitabine to the combination of fludarabine and busulfan, a widely used conditioning regimen in RIST (*4*, *17*), to suppress tumor progression before the emergence of a GVT effect, because pancreatic cancer progresses much faster than renal cell cancer. A synergistic antitumor effect with the combination of gemcitabine and fludarabine has been demonstrated in in vitro studies (*28*).

It can be difficult to distinguish between a chemotherapy effect and a GVT effect after RIST. In this study, however, a transient chemotherapy effect attributable to the conditioning regimen was observed as tumor marker regression during the first 2 weeks after RIST. Thereafter, tumor marker began to increase, which suggested that the chemotherapy effect did not persist for longer than 2 weeks. The second regression of tumor marker was observed at least 2 months after RIST, associated with the discontinuation of CsA, the development of GVHD, or DLI. An objective tumor response was also observed at least 2 months after RIST. Therefore, the GVT effect

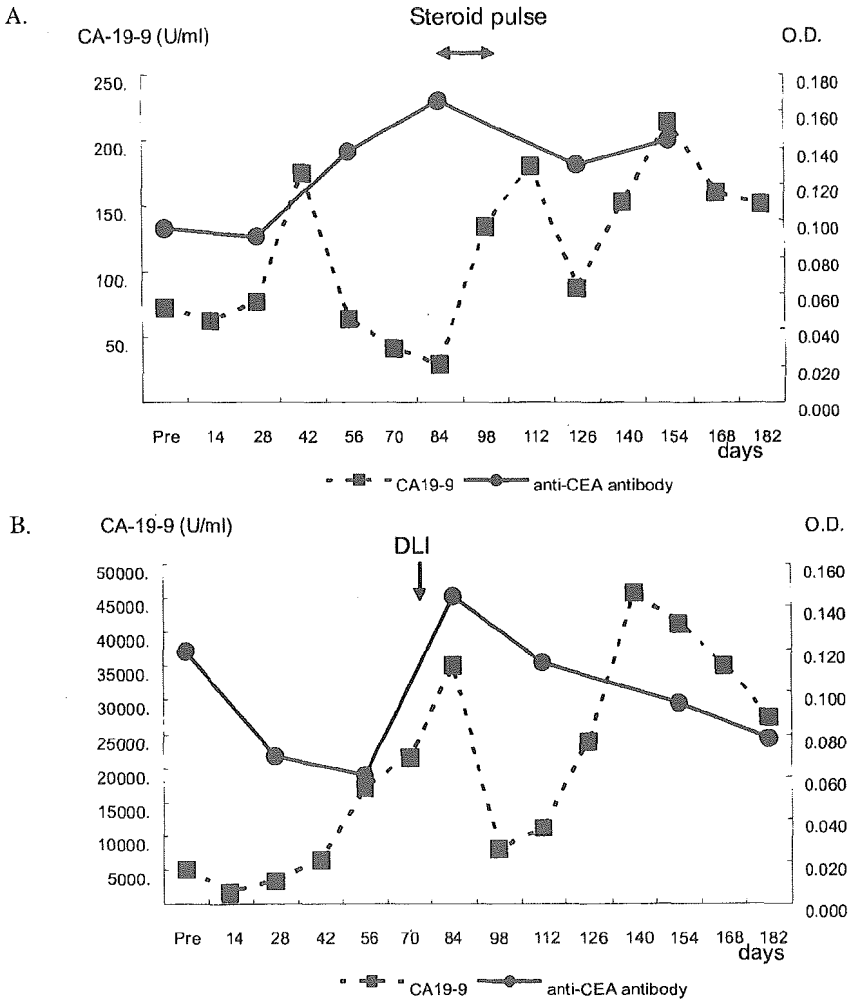

FIGURE 4. Serial changes in the serum CA19-9 level and anti-CEA antibody level. (A) Patient 5, who achieved a partial response on tumor marker evaluation. (B) Patient 6, who showed a tumor response after DLI.

against pancreatic cancer was clearly distinguished from the chemotherapy effect in this study.

Although a GVT effect against pancreatic cancer was seen in this study, this effect did not persist for more than 3 months. In addition, the development of GVHD was required to achieve a GVT effect. Therefore, we need a strategy for maintaining the GVT effect for a longer period without aggravating GVHD. To accomplish this, a specific immunotherapy against pancreatic cancer is required. Candidate target antigens include CA19-9, CA242, CEA, Her-2, mutated K-ras, and MUC-1 (*29*). Among these, CEA is attractive, because it is expressed in 85% to 90% of pancreatic cancer (*29*), and a specific immunotherapy against CEA could also be applied to other gastrointestinal cancers. Therefore, we retrospectively measured serial serum anti-CEA antibody levels in these patients. An increase in the serum anti-CEA antibody level after a transient decline just after RIST was associated with a tumor response. An elevation of serum anti-CEA antibody levels has already been demonstrated after a vaccine therapy targeting CEA (*23, 30*). Also, the presence of anti-CEA antibody at diagnosis was associated with better survival in patients with colon cancer, and thus anti-CEA antibody was suggested to have biologic significance (*31*). Thus, the GVT effect against pancreatic cancer in this study might be in part attributable to the specific immunity against CEA antigen. We also tried to detect CEA-specific cytotoxic T cells by enzyme-linked immunospot assay, but failed, probably because of the use of frozen peripheral blood mononuclear cells.

A major difference between RIST for hematologic malignancies and that for pancreatic cancer is the complications after transplantation. One patient (patient 1) experienced repeated episodes of biliary stent obstruction and bacterial cholangitis. Another two patients (patients 2 and 7) developed intestinal obstruction, probably because of the pancreatic head tumor. Therefore, a clinical trial of RIST for pancreatic cancer should be performed in close cooperation with the transplantation staff and gastroenterologists.

CONCLUSION

RIST appeared to be a feasible treatment for patients with advanced pancreatic cancer. The existence of a GVT effect against pancreatic cancer was strongly suggested by this study, but this effect was not durable and required the development of GVHD. We need to refine the strategy, for example, by the combination of specific immunotherapy against CEA after RIST.

REFERENCES

1. Burris HA III, Moore MJ, Andersen J, et al. Improvements in survival and clinical benefit with gemcitabine as first-line therapy for patients with advanced pancreas cancer: A randomized trial. *J Clin Oncol* 1997; 15: 2403.
2. Giralt S, Estey E, Albitar M, et al. Engraftment of allogeneic hematopoietic progenitor cells with purine analog-containing chemotherapy: Harnessing graft-versus-leukemia without myeloablative therapy. *Blood* 1997; 89: 4531.
3. Khouri IF, Keating M, Korbling M, et al. Transplant-lite: Induction of graft-versus-malignancy using fludarabine-based nonablative chemotherapy and allogeneic blood progenitor-cell transplantation as treatment for lymphoid malignancies. *J Clin Oncol* 1998; 16: 2817.
4. Slavin S, Nagler A, Naparstek E, et al. Nonmyeloablative stem cell transplantation and cell therapy as an alternative to conventional bone marrow transplantation with lethal cytoreduction for the treatment of malignant and nonmalignant hematologic diseases. *Blood* 1998; 91: 756.
5. Childs R, Clave E, Contentin N, et al. Engraftment kinetics after nonmyeloablative allogeneic peripheral blood stem cell transplantation: Full donor T-cell chimerism precedes alloimmune responses. *Blood* 1999; 94: 3234.
6. Saito T, Kanda Y, Kami M, et al. Therapeutic potential of a reduced-intensity preparative regimen for allogeneic transplantation with cladribine, busulfan, and antithymocyte globulin against advanced/refractory acute leukemia/lymphoma. *Clin Cancer Res* 2002; 8: 1014.
7. Eibl B, Schwaighofer H, Nachbaur D, et al. Evidence for a graft-versus-tumor effect in a patient treated with marrow ablative chemotherapy and allogeneic bone marrow transplantation for breast cancer. *Blood* 1996; 88: 1501.
8. Bay JO, Fleury J, Choufi B, et al. Allogeneic hematopoietic stem cell transplantation in ovarian carcinoma: Results of five patients. *Bone Marrow Transplant* 2002; 30: 95.
9. Childs R, Chernoff A, Contentin N, et al. Regression of metastatic renal-cell carcinoma after nonmyeloablative allogeneic peripheral-blood stem-cell transplantation. *N Engl J Med* 2000; 343: 750.
10. Rini BI, Zimmerman T, Stadler WM, et al. Allogeneic stem-cell transplantation of renal cell cancer after nonmyeloablative chemotherapy: Feasibility, engraftment, and clinical results. *J Clin Oncol* 2002; 20: 2017.
11. Bregni M, Dodero A, Peccatori J, et al. Nonmyeloablative conditioning followed by hematopoietic cell allografting and donor lymphocyte infusions for patients with metastatic renal and breast cancer. *Blood* 2002; 99: 4234.
12. Pedrazzoli P, Da Prada GA, Giorgiani G, et al. Allogeneic blood stem cell transplantation after a reduced-intensity, preparative regimen: A pilot study in patients with refractory malignancies. *Cancer* 2002; 94: 2409.
13. Ueno NT, Cheng YC, Rondon G, et al. Rapid induction of complete donor chimerism by the use of a reduced-intensity conditioning regimen composed of fludarabine and melphalan in allogeneic stem-cell transplantation for metastatic solid tumors. *Blood* 2003; 102: 3829.
14. Blaise D, Bay JO, Faucher C, et al. Reduced-intensity preparative regimen and allogeneic stem cell transplantation for advanced solid tumors. *Blood* 2004; 103: 435.
15. Childs R, Bradstock K, Gottlieb D, et al. Non-myeloablative allogeneic stem cell transplantation (NST) for metastatic melanoma: Nondurable chemotherapy responses without clinically meaningful graft-vs-tumor (GVT) effects. *Blood* 2002; 100: 429a.
16. Touroutoglou N, Gravel D, Raber MN, et al. Clinical results of a pharmacodynamically-based strategy for higher dosing of gemcitabine in patients with solid tumors. *Ann Oncol* 1998; 9: 1003.
17. Niiya H, Kanda Y, Saito T, et al. Early full donor myeloid chimerism after reduced-intensity stem cell transplantation using a combination of fludarabine and busulfan. *Haematologica* 2001; 86: 1071.
18. Przepiorka D, Weisdorf D, Martin P, et al. 1994 Consensus Conference on Acute GVHD Grading. *Bone Marrow Transplant* 1995; 15: 825.
19. Kanda Y, Mineishi S, Saito T, et al. Long-term low-dose acyclovir against varicella-zoster virus reactivation after allogeneic hematopoietic stem cell transplantation. *Bone Marrow Transplant* 2001; 28: 689.
20. Kanda Y, Mineishi S, Saito T, et al. Response-oriented preemptive therapy against cytomegalovirus disease with low-dose ganciclovir: A prospective evaluation. *Transplantation* 2002; 73: 568.
21. Kanda Y, Mineishi S, Saito T, et al. Pre-emptive therapy against cytomegalovirus (CMV) disease guided by CMV antigenemia assay after allogeneic hematopoietic stem cell transplantation: A single-center experience in Japan. *Bone Marrow Transplant* 2001; 27: 437.
22. Thiede C, Florek M, Bornhauser M, et al. Rapid quantification of mixed chimerism using multiplex amplification of short tandem repeat markers and fluorescence detection. *Bone Marrow Transplant* 1999; 23: 1055.
23. Conry RM, Allen KO, Lee S, et al. Human autoantibodies to carcinoembryonic antigen (CEA) induced by a vaccinia-CEA vaccine. *Clin Cancer Res* 2000; 6: 34.
24. Bearman SI, Appelbaum FR, Buckner CD, et al. Regimen-related toxicity in patients undergoing bone marrow transplantation. *J Clin Oncol* 1988; 6: 1562.
25. Aoki K, Okada S, Moriyama N, et al. Accuracy of computed tomography in determining pancreatic cancer tumor size. *Jpn J Clin Oncol* 1994; 24: 85.
26. Simon R. Optimal two-stage designs for phase II clinical trials. *Control Clin Trials* 1989; 10: 1.
27. Gooley TA, Leisenring W, Crowley J, et al. Estimation of failure probabilities in the presence of competing risks: New representations of old estimators. *Stat Med* 1999; 18: 695.
28. Plunkett W, Huang P, Xu YZ, et al. Gemcitabine: Metabolism, mechanisms of action, and self-potentiation. *Semin Oncol* 1995; 22: 3.
29. Kaufman HL, Di Vito J Jr, Horig H. Immunotherapy for pancreatic cancer: Current concepts. *Hematol Oncol Clin North Am* 2002; 16: 159.
30. Foon KA, Chakraborty M, John WJ, et al. Immune response to the carcinoembryonic antigen in patients treated with an anti-idiotype antibody vaccine. *J Clin Invest* 1995; 96: 334.
31. Albanopoulos K, Armakolas A, Konstadoulakis MM, et al. Prognostic significance of circulating antibodies against carcinoembryonic antigen (anti-CEA) in patients with colon cancer. *Am J Gastroenterol* 2000; 95: 1056.

Notch1 oncoprotein antagonizes TGF-β/Smad-mediated cell growth suppression via sequestration of coactivator p300

Shigeo Masuda,[1] Keiki Kumano,[1] Kiyoshi Shimizu,[1] Yoichi Imai,[1] Mineo Kurokawa,[1] Seishi Ogawa,[1,2] Makoto Miyagishi,[3] Kazunari Taira,[3] Hisamaru Hirai[1] and Shigeru Chiba[1,4]

[1]Departments of Hematology, Oncology and Cell Therapy, and Transplantation Medicine, Graduate School of Medicine, University of Tokyo, 7-3-1 Hongo, Bunkyo-ku, Tokyo 113-8655, [2]Department of Regeneration Medicine, Graduate School of Medicine, University of Tokyo, 7-3-1 Hongo, Bunkyo-ku, Tokyo 113-8655, and [3]Department of Chemistry and Biotechnology, School of Engineering, University of Tokyo, 7-3-1 Hongo, Bunkyo-ku, Tokyo 113-8656, Japan

(Received February 24, 2005/Accepted March 16, 2005/Online publication May 16, 2005)

The Notch proteins constitute a family of transmembrane receptors that play a pivotal role in cellular differentiation, proliferation and apoptosis. Although it has been recognized that excess Notch signaling is potentially tumorigenic, little is known about precise mechanisms through which dysregulated Notch signaling induces neoplastic transformation. Here we demonstrate that Notch signaling has a transcriptional cross-talk with transforming growth factor-β (TGF-β) signaling, which is well characterized by its antiproliferative effects. TGF-β-mediated transcriptional responses are suppressed by constitutively active Notch1, and this inhibitory effect is canceled by introduction of transcriptional coactivator p300. We further show that this blockade of TGF-β signaling is executed by the sequestration of p300 from Smad3. Moreover, in a human cervical carcinoma cell line, CaSki, in which Notch1 is spontaneously activated, suppression of Notch1 expression with small interfering RNA significantly restores the responsiveness to TGF-β. Taken together, we propose that Notch oncoproteins promote cell growth and cancer development partly by suppressing the growth inhibitory effects of TGF-β through sequestrating p300 from Smad3. (*Cancer Sci* 2005; 96: 274–282)

The Notch pathway constitutes an evolutionarily conserved signaling pathway that mediates critical cell fate decisions, such as differentiation, proliferation and apoptosis.[1,2] In addition to the fact that Notch signaling plays pivotal roles in embryonic development, and post-embryonic growth and differentiation in multiple systems such as the immune system,[3,4] substantial evidence indicates that the constitutively activated forms of Notch family proteins are involved in tumorigenesis:[5–17] *Notch1/TAN-1* was originally identified as a recurrent chromosomal translocation, t(7;9)(q34; q34.3), in a human acute T-cell lymphoblastic leukemia,[5] resulting in the expression of an extracellular region-truncated form of Notch1 that is known to be constitutively active. The N-terminal truncated forms of the Notch1 and Notch2 proteins have been implicated in the transformation of rat kidney cells in cooperation with an adenoviral oncoprotein, E1A.[10,15] Activated forms of the Notch1[8] and Notch3 proteins[13] are capable of generating T-cell leukemia when retrovirally introduced into bone marrow cells that are transplanted into irradiated recipient mice. Also, *Int-3*, which encodes a truncated form of Notch4, has been shown to contribute to the generation of mammary carcinoma in mice.[6,11] Interestingly, recent reports have suggested that Notch1 is upregulated in Ras-transformed cells in which activation of Notch1 signaling is necessary to maintain the neoplastic phenotype.[18] Notch activation that causes human neoplasms has been shown to result not only from the truncation, based on the genetic aberration, but also Notch ligand stimulation,[18,19] suggesting that Notch activation without its own genetic abnormalities could be frequently involved in tumorigenesis.[20,21]

Despite rapidly accumulating information about the Notch signaling system, little is known about the mechanism through which excess Notch signaling triggers cellular transformation. One of the clues to this issue is the fact that Notch serves as an adaptor for molecules involved in transcriptional machinery, among which we focus on p300,[22] one of the most common transcriptional coactivator proteins.

The p300 protein interacts with molecules functioning in multiple signaling pathways. Transforming growth factor-β (TGF-β) also uses p300 through activated Smad3.[23,24] TGF-β inhibits proliferation of a wide range of cells including epithelial, endothelial and hematopoietic cells. It plays an important role in controlling tumor development, and its signaling constitutes one of the tumor-suppressor pathways.[25–27] Smads are a class of proteins that function as intracellular signaling effectors for the TGF-β superfamily, which includes TGF-β, activins and bone morphogenetic proteins (BMP).[28,29] Smad2 and Smad3 are directly phosphorylated by the type I TGF-β receptor in response to TGF-β, leading to formation of heteromeric complexes with Smad4, and are then translocated into the nucleus where they bind to the TGF-β-responsive regulatory sequences, either directly through the Smad-binding elements or in conjugation with other sequence-specific DNA-binding proteins.[30–32] It is suggested that p300 forms the bridge between the Smad complex and the transcriptional apparatus.

Here we show that constitutively active Notch1, consisting of the intracellular domain alone (ICN1), inhibits the antiproliferative activity of TGF-β via the sequestration of p300 from Smad3. We propose that conferring resistance to TGF-β signaling may, in part, be attributed to a mechanism of Notch-induced neoplastic transformation.

Materials and Methods

Plasmids. Expression vectors for Smad2-Flag, Smad3-Flag and Smad4-hemagglutinin A (Smad4-HA) were described previously (pCMV5/Smad2-Flag, pCMV5/Smad3-Flag and pCMV5/Smad4-HA).[33,34] p3TP-Lux, pcDNA3/TβRI(TD)-HA, pcDNA3/6Xmyc-Smad3 and pcDEF3/p300-Flag were kindly provided by K. Miyazono (University of Tokyo, Japan). pcDNA3/myc-ICN1 (amino acids 1747–2531 of mouse Notch1), pME18Sneo/myc-ICN, pTracerCMV/ICN1-Flag, pTracerCMV/ICN2-Flag and pTracerCMV/ICN3-Flag were described previously.[35,36] The C-terminal deletion constructs,

[4]To whom correspondence should be addressed. E-mail: schiba-tky@umin.ac.jp

 doi: 10.1111/j.1349-7006.2005.00048.x

pcDNA3/myc-RAMICΔC (1747–2193) and pcDNA3/myc-RAM/ANK (1747–2097), were made by digestion of pcDNA3/myc-ICN1 with *Eco*RI and *Xba*I (RAMICΔC), and with *Eco*RI and *Eco*RV (RAM/ANK), respectively. The ΔEP in-frame deletion of ICN1 was constructed by digesting pcDNA3/myc-ICN1 with *Pvu*II and *Eco*RI, and religating the plasmid. The EP mutant construct corresponds to the 2102LDE/AAA2104 mutation in the EP domain of ICN1 and was made by using an *in vitro* mutagenesis system (Stratagene). The TP-1-Luc reporter plasmid pGa981–6 was a gift from L. Strobl and U. Zimber-Strobl (GSF Institute for Clinical Molecular Biology, Germany). pEF-BOSneo-RBP-J (R218H) was kindly provided by T. Honjo (Kyoto University, Japan).

Cell culture and establishment of stable clones. HepG2, Mv1Lu, C2C12 and COS-7 cells were cultured at 37°C under 5% CO_2 in Dulbecco's modified Eagle's medium supplemented with 10% fetal calf serum (FCS). CHO(r) cells were maintained in alpha-minimal essential medium containing 10% FCS. CaSki cells were cultured in RPMI 1640 containing 10% FCS. To generate stable Mv1Lu clones overexpressing ICN1, myc-ICN1 subcloned into the pME18Sneo vector was transfected using SuperFect (Qiagen) according to the manufacturer's instructions. These cells were selected in medium containing G418 (800 μg/mL). G418-resistant clones were screened for expression of myc-ICN1 by Western blotting. Two independent clones with comparable expression levels were used in further assays.

Growth inhibition assay. The stable clones derived from Mv1Lu cells were plated in duplicate at a density of 5×10^3 per well in 96-well culture plates. After 12 h, cells were treated with increasing concentrations of TGF-β1 (R and D Systems) for 48 h. During the last 4 h, the cells were labeled with 2.5 μCi/mL [^{3}H]thymidine (Amersham Pharmacia Biotech). Thereafter, the incorporation of [^{3}H]thymidine was determined by liquid scintillation counting.

For RNA interference, CaSki cells were seeded at a density of 5×10^3 per well in a 96-well culture plate 24 h after transfection with small interfering RNA (siRNA). At 12 h after seeding the cells were treated with increasing concentrations of TGF-β for 48 h, after which time the [^{3}H]thymidine incorporation assay was carried as described above.

RNA interference. The siRNA against human Notch1, 5′-AAGGUGUCUUCCAGAUCCUGA-3′, was produced by Qiagen-Xeragon (Germantown). A non-silencing siRNA, 5′-AAUUCUCCGAACGUGUCACGU-3′ (Qiagen-Xeragon), was used as a control. At 24 h after CaSki cells (1×10^5 per well) were seeded in six-well plates, the cells were transfected with siRNA at a final concentration of 50 nM using Oligofectamine transfection reagent (Invitrogen) according to the manufacturer's instructions. The cells were lysed 48 h after transfection and were subjected to Western blotting or used for the thymidine incorporation assay as described above.

Luciferase assay. For analysis of luciferase activities, HepG2 cells were seeded in 12-well culture plates at a density of 4×10^4 per well. Cells were then transfected 12 h after seeding with various amounts of effector plasmids, together with the reporter plasmids, using SuperFect (Qiagen). As an internal control of transfection efficiency, a plasmid expressing β-galactosidase was cotransfected. The cells were harvested 48 h after transfection and assayed for luciferase activity. The data were normalized to β-galactosidase activity. Cells were treated with 1 ng/mL TGF-β1 for 48 h before harvesting.

Coimmunoprecipitation and Western blotting. COS-7 cells transiently transfected with the constructs were washed and lysed in TNE buffer (10 mM Tris-HCl [pH 7.8], 150 mM NaCl, 1 mM ethylenediaminetetracetic acid, 0.5% Nonidet P-40, 0.1% aprotinin, 1 mM phenylmethylsulfonylfluoride, 12.5 mM β-glycerophosphate, 1 mM Na_3VO_4 and protease inhibitor cocktail [Sigma; 1/50 volume]). For immunoprecipitation, total cell extracts were incubated with anti-p300 monoclonal antibody (Upstate Biotechnology) for 4 h at 4°C. The samples were then incubated with protein G Sepharose (Pharmacia Biotech) for 15 min at 4°C. Immunoprecipitates were washed five times with the TNE buffer, subjected to sodium dodecyl sulfate-polyacrylamide gel electrophoresis and analyzed by Western blotting with anti-myc antibody (9E10). Western blotting to detect intramembranously cleaved Notch1 was carried out using anticleaved Notch1 (Val 1744) antibody (Cell Signaling Technology).

Results

Active Notch1 inhibits the antiproliferative effects of TGF-β. To determine whether constitutively active Notch1 could affect the antiproliferative effects of TGF-β, we established several Mv1Lu cell lines that express ICN1 stably (N1-1 and N1-4), along with control clones (M-1 and M-2) (Fig. 1a). We carried out [^{3}H]thymidine-incorporation assays in the presence of various concentrations of TGF-β. Results are expressed as percentages relative to values obtained from control cultures in the absence of TGF-β. For example, at 1 ng/mL TGF-β, the relative [^{3}H]thymidine incorporation by M-1 and M-2 was 6.5 ± 1.0% and 5.9 ± 0.6%, respectively, while that by N1-1 and N1-4 was 21.6 ± 0.2% and 28.6 ± 0.7%, respectively (Fig. 1b). These results demonstrate that the growth of the mock clones was effectively inhibited by TGF-β, whereas the Mv1Lu clones that overexpress ICN1 showed reduced responsiveness to TGF-β.

Knockdown of active Notch1 expression by siRNA restores the antiproliferative effects of TGF-β. To further investigate the role of active Notch1 on the antiproliferative effects of TGF-β, we used a human cervical carcinoma cell line, CaSki. This line of cells

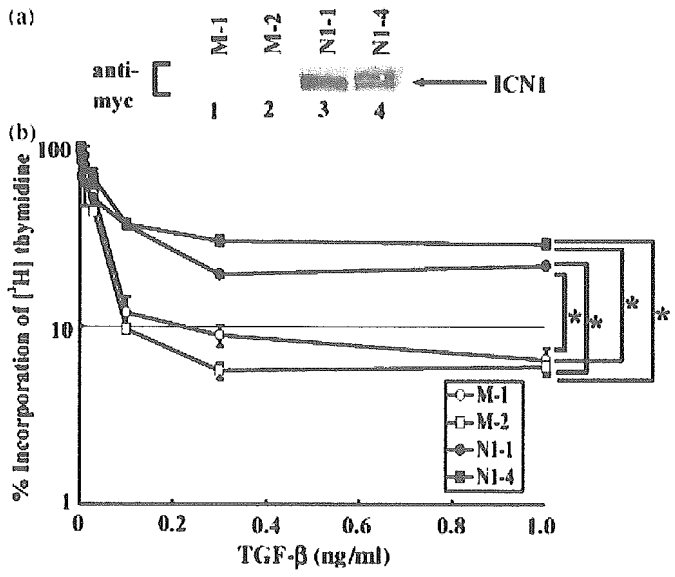

Fig. 1. Constitutive expression of active Notch1 (ICN1) in Mv1Lu cells overcomes transforming growth factor (TGF)-β-mediated growth inhibition. (a) Expression of ICN1 in stable Mv1Lu transfectants. Clones M-1 (lane 1) and M-2 (lane 2) are mock clones transfected with pME18Sneo empty vector followed by G418 selection. Clones N1-1 (lane 3) and N1-4 (lane 4) were established from cells transfected with pME18Sneo/myc-ICN1. The results of immunoblotting with anti-myc antibody are shown. (b) [^{3}H]thymidine incorporation into Mv1Lu clones was assayed in the presence of the indicated concentrations of TGF-β. Results are expressed as percentages relative to values obtained from control cultures in the absence of TGF-β. *$P < 0.01$.

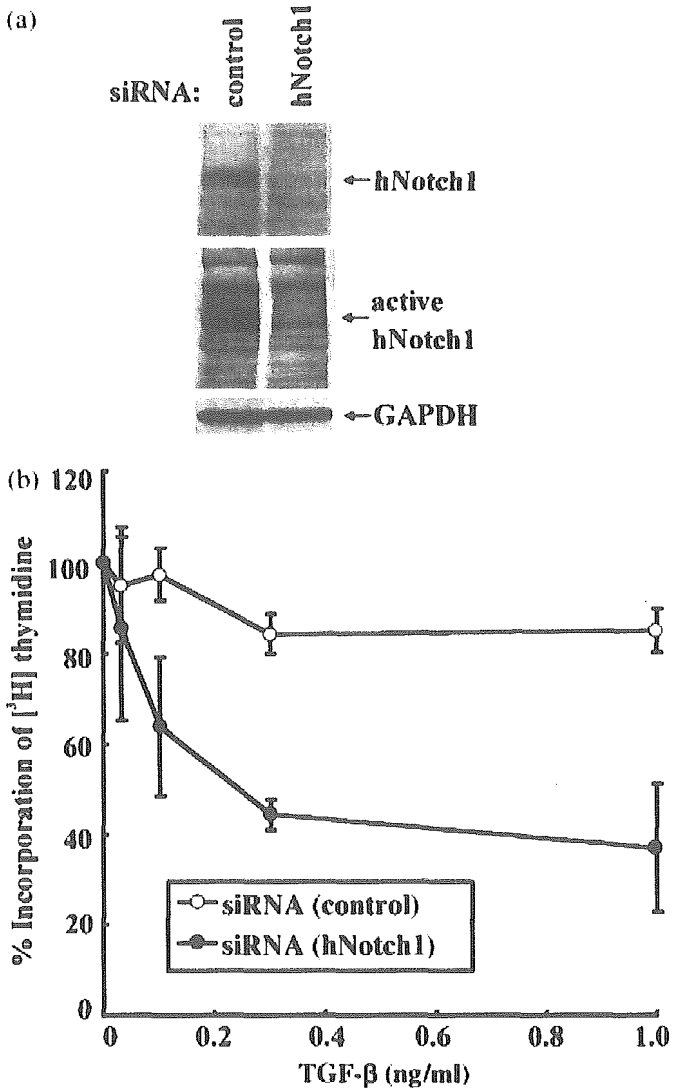

Fig. 2. Suppression of active Notch1 expression by small interfering RNA (siRNA) results in recovered responsiveness to transforming growth factor (TGF)-β. (a) Suppression of human Notch1 protein expression by siRNA. CaSki cells, spontaneously expressing truncated Notch1 protein, were transfected with control or human Notch1 siRNA, followed by immunoblotting. The upper panel, with antihuman Notch1 antibody (bTAN20); the middle panel, with anticleaved human Notch1 (Val 1744) antibody, specific to intramembranously truncated human Notch1; the lower panel, with anti-glyceraldehyde-3-phosphate dehydrogenase antibody as loading control. (b) [³H]Thymidine incorporation into CaSki cells, which had been transfected with control or human Notch1 (hNotch1) siRNA, was assayed in the presence of the indicated concentrations of TGF-β. Results are expressed as percentages relative to values obtained from control cultures in the absence of TGF-β.

has been shown to endogenously overexpress Notch1, leading to spontaneous activation of Notch1 (Fig. 2a).[18] Thus, this cell line could be useful for an approach based on siRNA. We transfected CaSki cells with siRNA targeted to human Notch1, which specifically and efficiently abrogated Notch1 protein expression (Fig. 2a). By using fluorescein-labeled control siRNA, we confirmed that siRNA could be introduced into CaSki cells with almost 100% efficiency (data not shown). Interestingly, an activated form of Notch1, which is detectable only by the antibody recognizing intramembranously cleaved Notch1, was undetectable if this siRNA was introduced (Fig. 2a). We found that wild-type and control siRNA-introduced CaSki cells had poor responsiveness to TGF-β, but after repression of active human Notch1 by siRNA, CaSki cells responded to TGF-β (Fig. 2b). Taken together, these results indicate that active Notch1 functions in CaSki cells to maintain their unresponsiveness to TGF-β.

Transcriptional responses mediated by TGF-β or Smad overexpression are suppressed by Notch signaling. Next, we examined the effects of ICN1 on TGF-β-mediated transcriptional responses in HepG2 cells with reporter assays using p3TP-Lux, a TGF-β-responsive reporter plasmid. Fold increase in the luciferase activity triggered by TGF-β was repressed to 20–30% when ICN1 was introduced (Fig. 3a).

To further investigate whether ligand-induced Notch signaling also represses TGF-β signaling, we used the C2C12 cell line, which is responsive to both Notch ligand[37] and TGF-β.[38] To stimulate cells with the Notch ligand Delta1, C2C12 cells were cocultivated with irradiated CHO(r) cells expressing full-length Delta1 (CHO-fD1).[39] The increase in luciferase activity of p3TP-Lux in the presence of TGF-β was repressed by Delta1 stimulation (Fig. 3b), suggesting that ligand-stimulated Notch signaling can antagonize TGF-β signaling.

We then examined whether ICN1 inhibits the transcriptional responses induced by Smad overexpression. Transcriptional activation of p3TP-Lux induced in HepG2 cells either by Smad3 alone or a combination of Smad2 or Smad3 with Smad4 was also suppressed by cotransfection with ICN1, in a dose-dependent manner (Fig. 3c,d). Similar repression was observed when we used other Smad-responsive reporter plasmids: p800neo-Luc, which contains the natural PAI-1 promoter, and p15P113-Luc, which contains the p15 promoter (Fig. 3e,f).

In vertebrates, Notch proteins comprise a family of four transmembrane receptors (Notch1 through Notch4).[1] To examine whether constitutively active Notch proteins other than ICN1 also inhibit TGF-β/Smad signaling, we compared the effect of ICN2 and ICN3 with that of ICN1 on the TGF-β-induced activation of the p3TP reporter. We found that ICN2 and ICN3 suppress TGF-β-induced transcriptional activation just as ICN1 did (Fig. 3g), indicating that suppression of TGF-β signaling is common to the constitutively active Notch proteins.

Overexpression of p300 partially overcomes the inhibitory effect of ICN1 on Smad3-mediated transactivation. Recent studies have indicated that both Smad proteins and ICN1 bind the general transcriptional coactivator p300 to mediate their transcriptional activities.[22–24] It is known that the binding regions of the p300 protein for the partner signaling molecules are variable and that both Smads and ICN1 bind the C-terminal region of p300. This information prompted us to examine whether p300 is involved in the Notch-mediated blockade of TGF-β/Smad signaling. When p300 was exogenously introduced into HepG2 cells, we observed that the ICN1-mediated suppression of Smad3-induced p3TP-Lux transactivation was reversed in a manner dependent on the dose of introduced p300 (Fig. 4).

These observations suggest that the availability of p300 by Smad3 may be limited and reduced when ICN1 is introduced. Therefore, we speculated that p300 may be sequestered from Smad3 by ICN1 when these molecules coexist. To see whether there is a reciprocal sequestration, we investigated whether ICN1-induced transcriptional activation of the TP-1 promoter, which is well characterized as a target of Notch signaling, is suppressed by the TGF-β/Smad activation. We observed a positive, although less remarkable, reciprocal repression of the ICN1-induced TP1 transactivation by overexpression of Smad3 and Smad4 (data not shown).

ICN1 mutants defective in p300 binding fail to repress the Smad-dependent transcriptional activation. Notch1 interacts with p300 through the 'EP domain' located at the C-terminal flanking region of the ankyrin repeats (ANK).[22] To further demonstrate that p300 is involved in the ICN1-mediated repression of TGF-β/Smad-induced transactivation, we used ICN1 mutants either

 doi: 10.1111/j.1349-7006.2005.00048.x

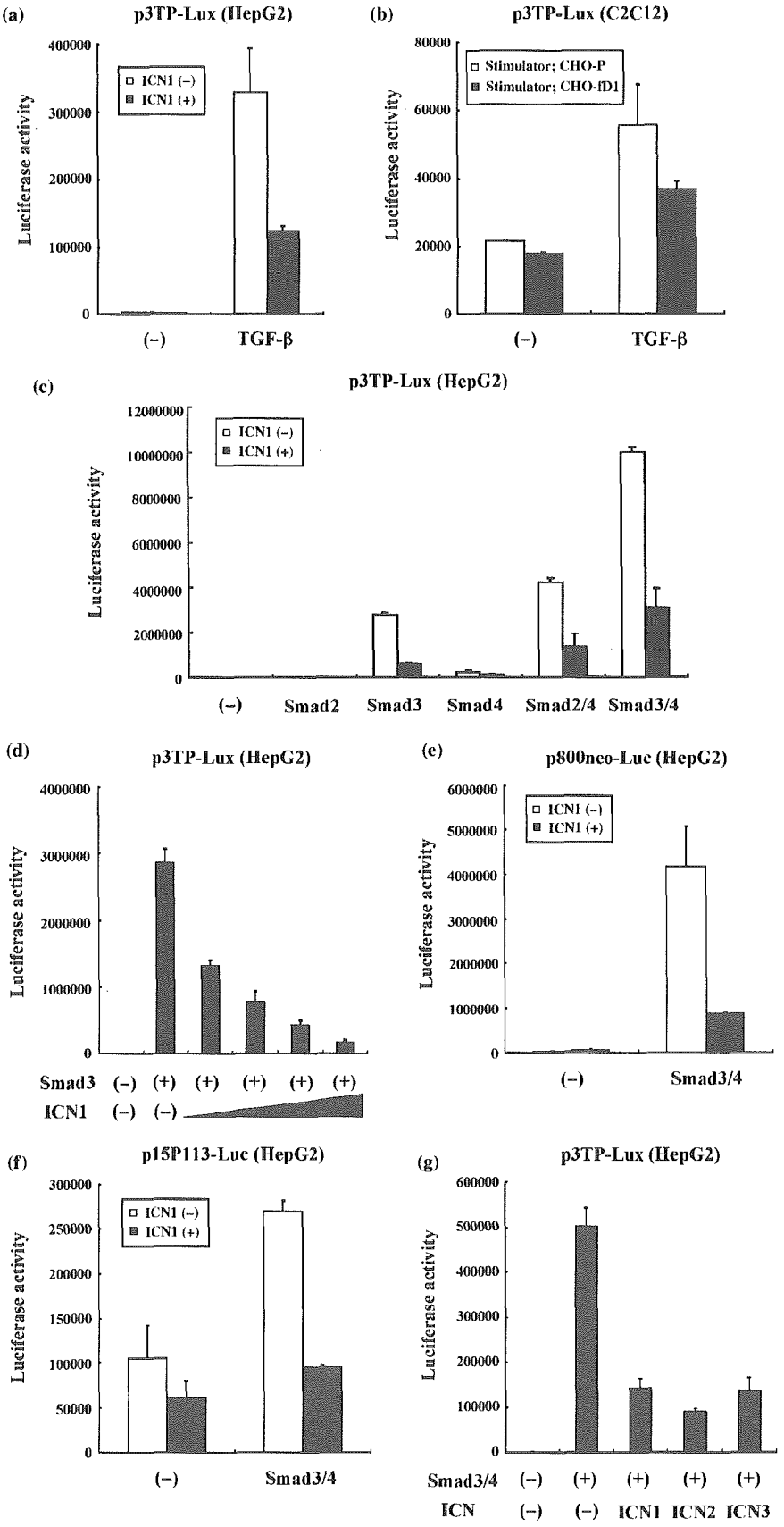

Fig. 3. Transforming growth factor (TGF)-β or Smad-mediated transcriptional responses are suppressed by Notch signaling. (a) TGF-β-induced transcriptional responses are repressed by ICN1. p3TP-Lux was transfected into HepG2 cells together with either pcDNA3 empty vector or pcDNA3-ICN1. Cells were incubated in the absence or presence of 1 ng/mL TGF-β for 48 h, and luciferase activities were measured. (b) Notch ligand stimulation also inhibits the TGF-β-mediated transcriptional responses. C2C12 cells, transiently transfected with p3TP-Lux, were cocultured with either irradiated parental CHO(r) cells (CHO-P) or irradiated CHO(r) cells expressing full-length Delta1 (CHO-fD1) in the absence or presence of 5 ng/mL TGF-β for 48 h, and luciferase activities were measured. (c) ICN-1 suppresses Smad-induced transcriptional responses. Either pcDNA3 empty vector or pcDNA3-ICN1, together with p3TP-Lux, was transfected into HepG2 cells, in combination with the indicated Smad constructs. (d) ICN1 represses Smad-induced responses in a dose-dependent manner. HepG2 cells were transfected with 3, 10, 30 or 100 ng ICN1 expression plasmid, together with p3TP-Lux and Smad3. Smad-induced transcriptional responses with (e) p800neo-Luc or (f) p15P113-Luc are also repressed by ICN1. p800neo-Luc or p15P113-Luc was transfected into HepG2 cells together with either pcDNA3 empty vector or pcDNA3-ICN1, in combination with Smad3 and Smad4. (g) ICN2 and ICN3 suppress the Smad-mediated transcriptional activation as ICN1. Either pTracerCMV empty vector, pTracerCMV/ICN1, pTracerCMV/ICN2 or pTracerCMV/ICN3 was transfected into HepG2 cells, together with p3TP-Lux, Smad3 and Smad4, and luciferase activities were measured.

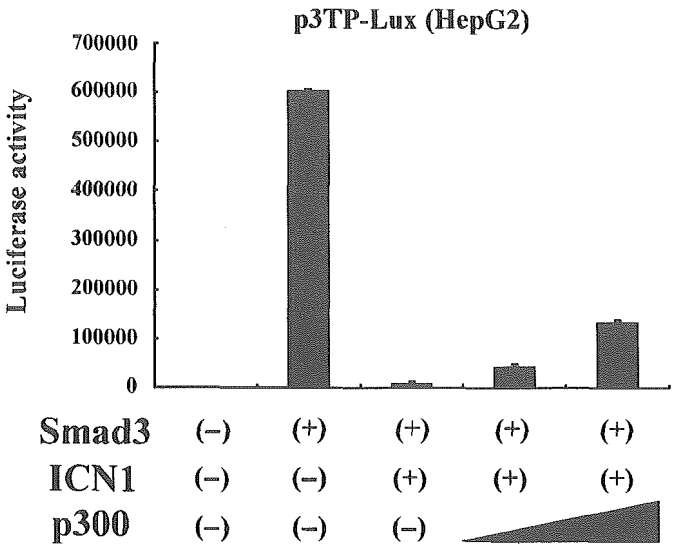

Fig. 4. Repression of Smad3-mediated transactivation by ICN1 is recovered with coactivator p300. Introduction of p300 partially rescues the ICN1-mediated suppression of Smad3-induced p3TP-Lux transactivation in a dose-dependent manner. HepG2 cells were transfected with 0.1 or 1 μg p300 expression plasmid, together with p3TP-Lux, Smad3 and ICN1, followed by a luciferase assay.

with or without the p300 interaction capability (Fig. 5a). RAMICΔC is a C-terminally truncated mutant that lacks the TAD and PEST domains but contains the EP domain. In RAM/ANK, the EP domain and all the sequence C-terminal to it are deleted. ΔEP is an internal deletion mutant lacking only 15 amino acids corresponding to the EP domain. EP (LDE/AAA) carries a three-amino acid substitution, i.e. LDE to AAA within the EP domain, which was previously demonstrated to be critical for transactivation of Notch signaling as well as for the interaction with p300.[22] As expected, RAM/ANK, ΔEP and EP (LDE/AAA), all of which lose the capacity to interact with p300, failed to fully repress transcription from the 3TP promoter induced by overexpression of Smad3 and Smad4. In contrast, RAMICΔC, which binds to p300, suppressed the TGF-β/Smad-induced transactivation just as wild-type ICN1 did (Fig. 5b). The expression levels of ICN1 and its derivatives in HepG2 cells were analyzed by Western blotting (Fig. 5b). These results suggest that the EP domain is required for the suppression of the Smad transactivation by ICN1.

ICN1 reduces the amount of p300 binding to Smad3. To determine whether ICN1 interferes with Smad3 activity through sequestration of p300, we investigated the effect of wild type and various mutants of ICN1 on the interaction between Smad3 and p300 in the presence of activated TGF-β receptor. As shown in previous reports,[24] we observed that Smad3 was coimmunoprecipitated with p300 (Fig. 6). The amount of coimmunoprecipitated Smad3, however, was markedly reduced when wild-type ICN1 was cotransfected. RAMICΔC showed a similar effect, whereas RAM/ANK, ΔEP and EP (LDE/AAA) had little or no effect on the amounts of Smad3 coprecipitated with p300 (Fig. 6). Taken together, these results suggest that the EP domain of ICN1 is essential for the sequestration of p300 from Smad3.

The RBP-J-dependent transcription of target genes is not required for the repression of TGF-β signaling by ICN1. If the inhibition of Smad3-mediated transcriptional activation by ICN1 is attributed

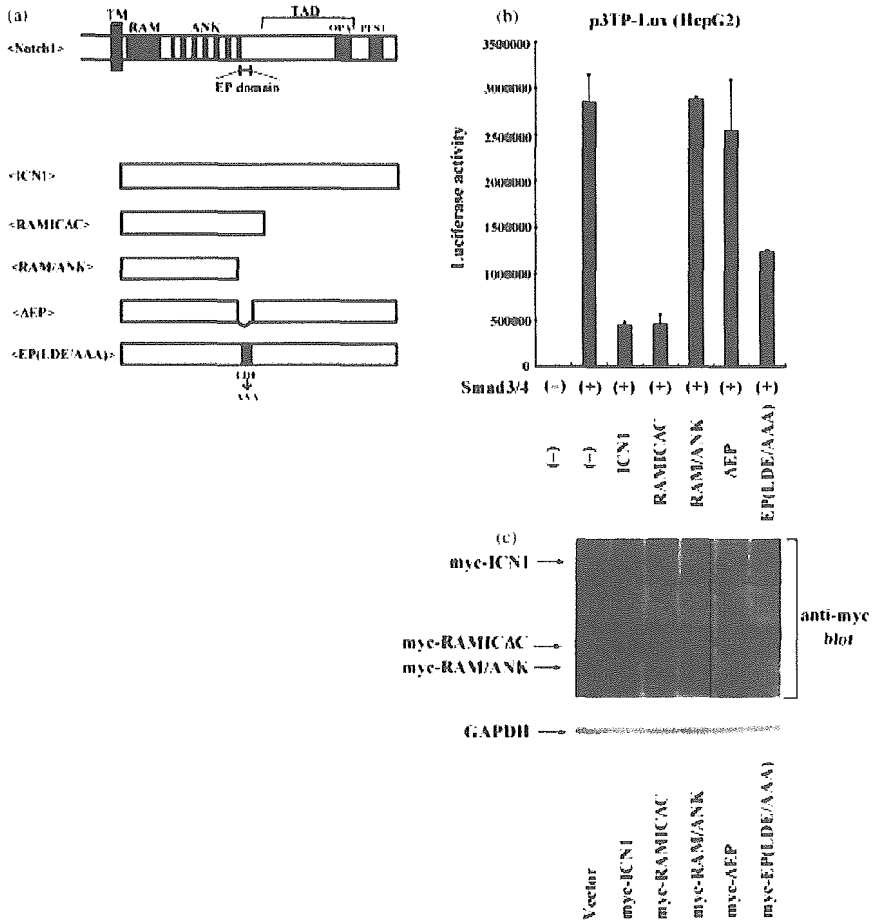

Fig. 5. The EP domain is indispensable for suppression of Smad signaling by ICN1. (a) Schematic representation of the mouse Notch1 intracellular region (ICN1) and its derivatives used in this study. The EP domain, essential for ICN1 to interact with p300, is located in the C-terminal flanking region adjacent to the ankyrin repeats of ICN1. (b) Structural requirements for repression of Smad signaling by ICN1. HepG2 cells were transfected with Smad3, Smad4 and p3TP-Lux together with wild type or each mutant of ICN1, and luciferase activities were measured. Expression levels of myc-ICN1 and its myc-tagged derivatives were evaluated in HepG2 cells. Each whole cell extract was analyzed by Western blotting using an anti-myc antibody (upper panel). The lower panel shows the glyceraldehyde-3-phosphate dehydrogenase expression as loading control.

 doi: 10.1111/j.1349-7006.2005.00048.x

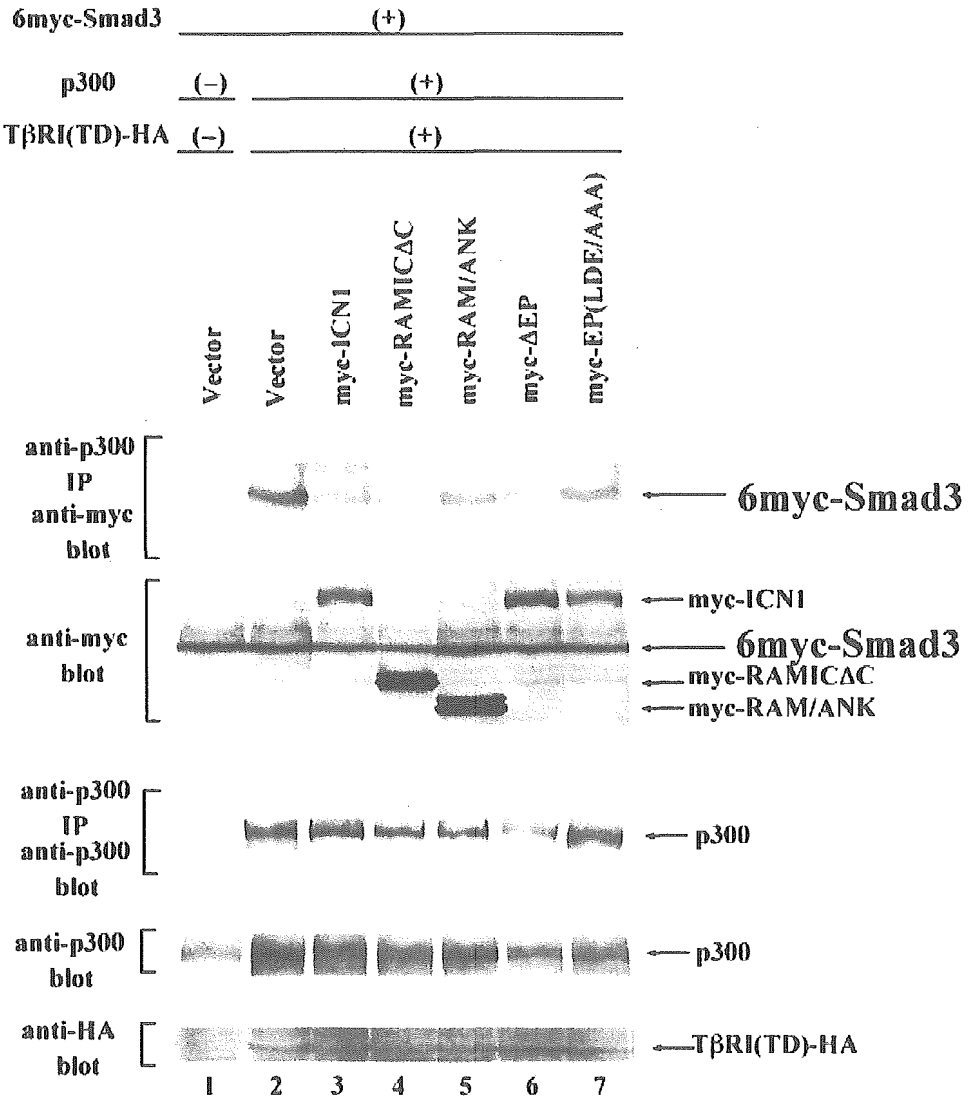

Fig. 6. Effects of ICN1 on the p300–Smad interaction. Wild type or each mutant of ICN1 was coexpressed in COS-7 cells with 6myc-Smad3, TβRI(TD)-HA and p300. The cell lysates of transfected COS-7 cells were subjected to immunoprecipitation with anti-p300 antibody followed by immunoblotting with anti-myc antibody, which detects the interaction of p300 and 6myc-Smad3. Immunoprecipitates were also blotted with anti-p300 antibody, and cell lysates were blotted with anti-myc, anti-p300 and anti-hemagglutinin A antibodies.

to the sequestration of p300 from Smad3, we hypothesized that it may not be mediated by transcription targeted by the complex of ICN1 and RBP-J (or CSL from *C*BF1/RBP-J, *S*uppressor of Hairless, *L*ag-1), a DNA-binding protein with which activated Notch proteins transactivate target genes. To clarify this possibility, we used a dominant-negative form of RBP-J (RBP-J [R218H];[40] hereafter referred to as DN-RBP), which lacks the ability to bind to DNA but still interacts with Notch1 and represses ICN1-induced transactivation of the TP-1 promoter (Fig. 7a). Reporter assays showed that DN-RBP did not reverse the ICN1-induced repression of TGF-β signaling, indicating that the RBP-J-dependent transcription of specific target genes is not required for ICN1-induced repression of TGF-β signaling (Fig. 7b).

Discussion

In this study, we have demonstrated a transcriptional cross-talk between the Notch and TGF-β signaling pathways. Because Smad proteins are important tumor suppressors, the ability of active Notch1 (ICN1) to repress TGF-β signaling could be responsible, at least partially, for the transforming activity of Notch. A recent study has reported that ICN1 blocks TGF-β-mediated growth arrest in epithelial cells.[41] In that context, ICN1 deregulates expression of c-Myc and thereby renders epithelial cells resistant to growth-inhibitory signals, suggesting a novel link between Notch and cell cycle control. In the experiments described here, we show another mechanism explaining the antagonism between the Notch and TGF-β signaling systems, that is, repression of TGF-β-mediated signaling through sequestration of coactivator p300 by ICN1, which is apparently independent from the mechanism demonstrated by Rao and Kadesch.[41]

Importantly, some investigators have demonstrated that Notch and Smad signaling show functional synergism.[42–44] More complexly, transcriptional activation of the hairy/enhancer of split (HES)-related gene Hey1 is both a direct target of Smad3 and an indirect target through Smad3-dependent transcriptional activation of Notch signaling component genes.[45] Demonstration of direct and TGF-β-dependent interactions between Smad3 and ICN1,[44] and Smad1/5 and ICN1,[42,43] indeed serves as bona-fide evidence of the cross-talk between these two signaling

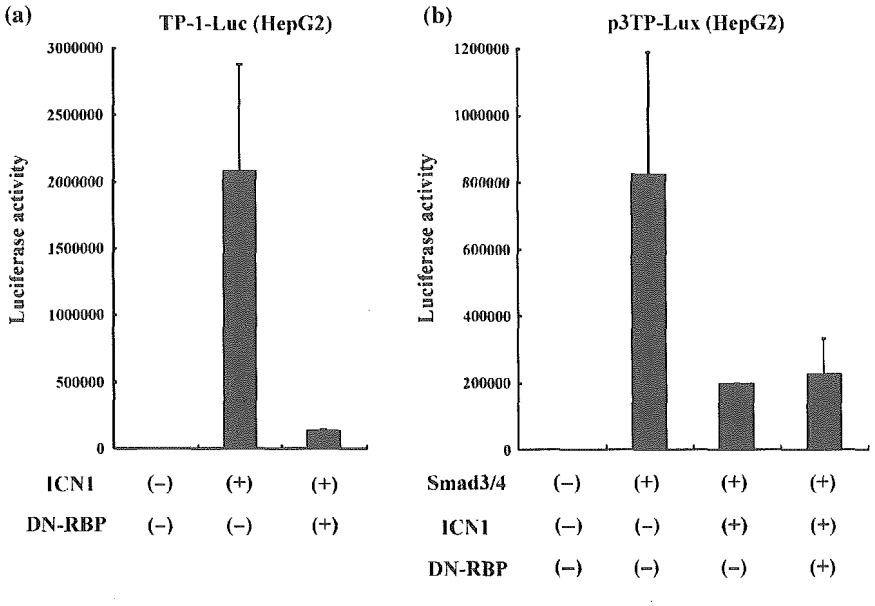

Fig. 7. The effects of DN-RBP on the transcriptional activity of ICN1 and the Smad proteins. (a) Expression of a dominant-negative form of RBP-J (DN-RBP) suppresses TP-1 activity induced by ICN1. TP-1-Luc was transfected into HepG2 cells, together with ICN1 and DN-RBP. (b) DN-RBP does not reverse the ICN1-induced repression of the Smad signaling. p3TP-Lux was transfected into HepG2 cells, together with Smad3, Smad4, ICN1 and DN-RBP.

systems. It appears that various molecular interactions could exist between these two signaling systems, most likely in a cell context-dependent manner. Indeed, there is a report showing that both synergy and antagonism could occur between the Notch and Smad signaling systems.[43]

Many transcription factors, including ICN1 and Smads, use the coactivator p300 to activate transcription.[22–24] The p300 protein is generally present at limiting concentrations within the cell nucleus, and functional antagonism between transcription factors occurs as a consequence of direct competition for binding to p300.[46–50] Domains within the p300 protein for interaction with individual transcription factors are highly variable, but both active Notch1 and Smad have been reported to bind to the C-terminal domain, which can potentially be shared. Our results suggest competition between active Notch1 and Smad for limiting quantities of complexes containing p300. Similar competition for p300 has been described for several cellular pathways, including nuclear receptor and AP-1,[46] p53 and E2F,[47] NF-κB and p53,[48] NF-κB and nuclear receptor,[49] and STAT and AP-1.[50]

Regarding Notch-induced transformation, previous studies have indicated that in baby rat kidney cells (RKE) immortalized with E1A, the minimal transforming domain includes ANK and flanking 107 C-terminal amino acids.[15] Consistent with this, our data showed that the EP domain, adjacent to ANK, is required for suppressing Smad activity by ICN1. Recently, the crystal structure revealed that the LDE motif in the EP domain not only governs the stability around this domain but also potentially contributes to direct contacts with p300,[51] supporting our result that the EP mutant (LDE/AAA) fails to sequester p300 from Smad3. Moreover, it is interesting that p300 was isolated as a cellular target of the adenoviral oncoprotein E1A,[52] which is known to block the functions of p300. Therefore, we can speculate that ICN1 may promote sequestration of p300 from Smad3 in cooperation with E1A in RKE cells.

In this study, the biological phenomenon under this transcriptional cross-talk was assessed by both upregulation and downregulation of Notch signaling. For the former, we used strategies of ligand stimulation and overexpression of constitutively active Notch1. For the latter, siRNA-based suppression of Notch1 synthesis in CaSki cells was used successfully to significantly reduce spontaneous generation of the cleaved (i.e. active form of) Notch1. We can speculate that Notch1 is spontaneously activated in CaSki cells either by ligand stimulation from neighboring cells or a cell-autonomous mechanism. In either case, we have demonstrated that spontaneous activation of Notch1 contributes to the growth of CaSki cells, and that blockade of this activation results in a recovered responsiveness to TGF-β. Taken together, we have here demonstrated that active Notch1 may serve as a positive regulator of cell growth by repressing TGF-β-induced growth inhibition. We observed, however, that CaSki cells made no response to TGF-β under treatment with γ-secretase inhibitors, chemical compounds that block Notch cleavage, despite our observation that the amount of active Notch1 was decreased and the transcriptional activation of the Notch reporter gene was suppressed when CaSki cells were treated with γ-secretase inhibitors (data not shown). This observation was apparently puzzling. However, it has since been reported that many transmembrane proteins, in addition to Notch and the amyloid precursor protein that was the substrate identified originally, could be substrates of the γ-secretase.[53] These new lines of evidence made it possible for us to speculate that γ-secretase inhibitors might influence other growth signal pathways and that the specific knockdown of Notch signaling might be achieved using the RNA interference technique, rather than with a γ-secretase inhibitor. It is of future interest to elucidate the mechanisms underlying the failure to restore responsiveness to TGF-β by γ-secretase inhibitors in CaSki cells.

Genetic and molecular studies have implicated several downstream components in the Notch signaling pathway, such as RBP-J and Deltex. As RBP-J is one of the main effectors in Notch signaling,[37,54] it is critical to determine whether the RBP-J-dependent transcription is required for the inhibitory effect of Notch signaling. If that is the case, DN-RBP, a DNA-binding mutant that perturbs Notch activity in a dominant-negative manner, should cancel this suppression. The negative result of the experiment using DN-RBP, however, suggests that RBP-J-dependent transcription of specific target genes is not required for the inhibition of TGF-β signaling.

The p300 protein functions as global transcriptional coactivator and plays important roles in a broad spectrum of biological processes, including cell proliferation and differentiation.[52] A role for p300 in tumor suppression has been proposed, and biallelic mutations of p300 have been identified in certain types of human cancers.[55,56] Furthermore, it was reported recently that reintroduction of wild-type p300 suppresses the growth of p300-deficient carcinoma cells.[57] Insufficiency of cyclic AMP response element binding protein (CBP), a coactivator closely

 doi: 10.1111/j.1349-7006.2005.00048.x

related to p300, also results in both Rubinstein–Taybi Syndrome in humans, a disease characterized by an increased propensity for malignancies, and an increased incidence of leukemias in mice, suggesting that characteristics of tumor suppressors may be common to these general coactivators p300 and CBP.[52]

In summary, we propose that activated Notch represses TGF-β-mediated signaling possibly through sequestration of coactivator p300, which contributes to the mechanisms of Notch-induced neoplastic transformation. Our current results indicate that Notch oncoproteins promote cell proliferation and tumor development partly by repressing the tumor suppressor Smad.

Acknowledgments

We thank K. Miyazono for p3TP-Lux, pcDNA3/TβRI(TD)-HA, pcDNA3/6Xmyc-Smad3 and pcDEF3/p300-Flag; J. L. Wrana for Flag-Smad2; R. Derynck for Flag-Smad3 and Flag-Smad4; T. Honjo for pEF-BOSneo-RBP-J (R218H); L. Strobl and U. Zimber-Strobl for pGa986-1. We are also grateful to C. Kato for her technical help. This work was supported in part by grants-in-aid (KAKENHI, numbers 13307029 and 14370300) and Special Coordination Funds for Promoting Science and Technology from the Ministry of Education, Culture, Sports, Science and Technology of Japan, and Health and Labor Sciences Research Grants (Research Grants on Pharmaceutical and Medical Safety) from the Ministry of Health, Labor and Welfare of Japan.

References

1 Artavanis-Tsakonas S, Rand MD, Lake R. Notch signaling: cell fate control and signal integration in development. *Science* 1999; **284**: 770–6.
2 Allman D, Punt JA, Izon DJ, Aster JC, Pear WS. An invitation to T and more: Notch signaling in lymphopoiesis. *Cell* 2002; **109**: S1–11.
3 Pui JC, Allman D, Xu L, DeRocco S, Karnell FG, Bakkour S, Lee JY, Kadesch T, Hardy RR, Aster JC, Pear WS. Notch1 expression in early lymphopoiesis influences B versus T lineage determination. *Immunity* 1999; **11**: 299–308.
4 Radtke F, Wilson A, Stark G, Bauer M, van Meerwijk J, MacDonald HR, Aguet M. Deficient T cell fate specification in mice with an induced inactivation of Notch1. *Immunity* 1999; **10**: 547–58.
5 Ellisen LW, Bird J, West DC, Soreng AL, Reynolds TC, Smith SD, Sklar J. TAN-1, the human homolog of the Drosophila notch gene, is broken by chromosomal translocations in T lymphoblastic neoplasms. *Cell* 1991; **66**: 649–61.
6 Robbins J, Blondel BJ, Gallahan D, Callahan R. Mouse mammary tumor gene int-3: a member of the notch gene family transforms mammary epithelial cells. *J Virol* 1992; **66**: 2594–9.
7 Aster JC, Pear WS, Hasserjian RP, Erba H, Davi F, Luo B, Scott M, Baltimore D, Sklar J. Functional analysis of the TAN-1 gene, a human homolog of Drosophila notch. *Cold Spring Harbor Symp Quant Biol* 1994; **59**: 125–36.
8 Pear WS, Aster JC, Scott ML, Hasserjian RP, Soffer B, Sklar J, Baltimore D. Exclusive development of T cell neoplasms in mice transplanted with bone marrow expressing activated Notch alleles. *J Exp Med* 1996; **183**: 2283–91.
9 Aster JC, Robertson ES, Hasserjian RP, Turner JR, Kieff E, Sklar J. Oncogenic forms of NOTCH1 lacking either the primary binding site for RBP-J or nuclear localization sequences retain the ability to associate with RBP-J and activate transcription. *J Biol Chem* 1997; **272**: 11 336–43.
10 Capobianco AJ, Zagouras P, Blaumueller CM, Artavanis-Tsakonas S, Bishop JM. Neoplastic transformation by truncated alleles of human NOTCH1/TAN1 and NOTCH2. *Mol Cell Biol* 1997; **17**: 6265–73.
11 Gallahan D, Callahan R. The mouse mammary tumor associated gene INT3 is a unique member of the NOTCH gene family (NOTCH4). *Oncogene* 1997; **14**: 1883–90.
12 Aster JC, Xu L, Karnell FG, Patriub V, Pui JC, Pear WS. Essential roles for ankyrin repeat and transactivation domains in induction of T-cell leukemia by Notch1. *Mol Cell Biol* 2000; **20**: 7505–15.
13 Bellavia D, Campese AF, Alesse E, Vacca A, Felli MP, Balestri A, Stoppacciaro A, Tiveron C, Tatangelo L, Giovarelli M, Gaetano C, Ruco L, Hoffman ES, Hayday AC, Lendahl U, Frati L, Gulino A, Screpanti I. Constitutive activation of NF-κB and T-cell leukemia/lymphoma in Notch3 transgenic mice. *EMBO J* 2000; **19**: 3337–48.
14 Dumont E, Fuchs KP, Bommer G, Christoph B, Kremmer E, Kempkes B. Neoplastic transformation by Notch is independent of transcriptional activation by RBP-J signalling. *Oncogene* 2000; **19**: 556–61.
15 Jeffries S, Capobianco AJ. Neoplastic transformation by Notch requires nuclear localization. *Mol Cell Biol* 2000; **20**: 3928–41.
16 Aster JC, Pear WS. Notch signaling in leukemia. *Curr Opin Hematol* 2001; **8**: 237–44.
17 Weng AP, Ferrando AA, Lee W, Morris JP, Silverman LB, Sanchez-Irizarry C, Blacklow SC, Look T, Aster JC. Activating mutations of *NOTCH1* in human T cell acute lymphoblastic leukemia. *Science* 2004; **306**: 269–71.
18 Weijzen S, Rizzo P, Braid M, Vaishnav R, Jonkheer SM, Zlobin A, Osborne BA, Gottipati S, Aster JC, Hahn WC, Rudolf M, Siziopikou K, Kast WM, Miele L. Activation of Notch-1 signaling maintains the neoplastic phenotype in human Ras-transformed cells. *Nat Med* 2002; **8**: 979–86.
19 Yan XQ, Sarmiento U, Sun Y, Huang G, Guo J, Van Juan TG, Qi MY, Scully S, Senaldi G, Fletcher FA. A novel Notch ligand, Dll4, induces T-cell leukemia/lymphoma when overexpressed in mice by retroviral-mediated gene transfer. *Blood* 2001; **98**: 3793–9.
20 Zagouras P, Stifani S, Blaumueller CM, Carcangiu ML, Artavanis-Tsakonas S. Alterations in Notch signaling in neoplastic lesions of the human cervix. *Proc Natl Acad Sci USA* 1995; **92**: 6414–18.
21 Jundt F, Anagnostopoulos I, Forster R, Mathas S, Stein H, Dorken B. Activated Notch1 signaling promotes tumor cell proliferation and survival in Hodgkin and anaplastic large cell lymphoma. *Blood* 2002; **99**: 3398–403.
22 Oswald F, Täuber B, Dobner T, Bourteele S, Kostezka U, Adler G, Liptay S, Schmid RM. p300 acts as a transcriptional coactivator for mammalian Notch-1. *Mol Cell Biol* 2001; **21**: 7761–74.
23 Nishihara A, Hanai J-I, Okamoto N, Yanagisawa J, Kato S, Miyazono K, Kawabata M. Role of p300, a transcriptional coactivator, in signalling of TGF-β. *Genes Cells* 1998; **3**: 613–23.
24 Pouponnot C, Jayaraman L, Massague J. Physical and functional interaction of Smads and p300/CBP. *J Biol Chem* 1998; **273**: 22 865–8.
25 Massague J, Blain SW, Lo RS. TGF-β signaling in growth control, cancer, and heritable disorders. *Cell* 2000; **103**: 295–309.
26 Derynck R, Akhurst RJ, Balmain A. TGF-β signaling in tumor suppression and cancer progression. *Nat Genet* 2001; **29**: 117–29.
27 Wakefield LM, Roberts AB. TGF-β signaling. positive and negative effects on tumorigenesis. *Curr Opin Genet Dev* 2002; **12**: 22–9.
28 Heldin CH, Miyazono K, ten Dijke P. TGF-β signalling from cell membrane to nucleus through SMAD proteins. *Nature* 1997; **390**: 465–71.
29 Chang H, Brown CW, Matzuk MM. Genetic analysis of the mammalian transforming growth factor-β superfamily. *Endo Rev* 2002; **23**: 787–823.
30 Nakao A, Imamura T, Souchelnytskyi S, Kawabata M, Ishisaki A, Oeda E, Tamaki K, Hanai J, Heldin CH, Miyazono K, ten Dijke P. TGF-β receptor-mediated signaling through Smad2, Smad3 and Smad4. *EMBO J* 1997; **16**: 5353–62.
31 Massague J. How cells read TGF-β signals. *Nat Rev Mol Cell Biol* 2000; **1**: 169–78.
32 Massague J, Chen YG. Controlling TGF-β signaling. *Genes Dev* 2000; **14**: 627–44.
33 Kurokawa M, Mitani K, Irie K, Matsuyama T, Takahashi T, Chiba S, Yazaki Y, Matsumoto K, Hirai H. The oncoprotein Evi-1 represses TGF-β signalling by inhibiting Smad3. *Nature* 1998; **394**: 92–6.
34 Imai Y, Kurokawa M, Izutsu K, Hangaishi A, Maki K, Ogawa S, Chiba S, Mitani K, Hirai H. Mutations of Smad4 gene in acute myelogeneous leukemia and their functional implications in leukemogenesis. *Oncogene* 2001; **20**: 88–96.
35 Kumano K, Chiba S, Shimizu K, Yamagata T, Hosoya N, Saito T, Takahashi T, Hamada Y, Hirai H. Notch1 inhibits differentiation of hematopoietic cells by sustaining GATA-2 expression. *Blood* 2001; **98**: 3283–9.
36 Shimizu K, Chiba S, Saito T, Kumano K, Hamada Y, Hirai H. Functional diversity among Notch1, Notch2, and Notch3 receptors. *Biochem Biophys Res Commun* 2002; **291**: 775–9.
37 Nofziger D, Miyamoto A, Lyons KM, Weinmaster G. Notch signaling imposes two distinct blocks in the differentiation of C2C12 myoblasts. *Development* 1999; **126**: 1689–702.
38 Liu D, Black BL, Derynck R. TGF-β inhibits muscle differentiation through functional repression of myogenic transcription factors by Smad3. *Genes Dev* 2001; **15**: 2950–66.
39 Shimizu K, Chiba S, Hosoya N, Kumano K, Saito T, Kurokawa M, Kanda Y, Hamada Y, Hirai H. Binding of Delta1, Jagged1, and Jagged2 to Notch2 rapidly induces cleavage, nuclear translocation, and hyperphosphorylation of Notch2. *Mol Cell Biol* 2000; **20**: 6913–22.
40 Chung CN, Hamaguchi Y, Honjo T, Kawaichi M. Site-directed mutagenesis study on DNA binding regions of the mouse homologue of Suppressor of Hairless, RBP-Jκ. *Nucl Acids Res* 1994; **22**: 2938–44.
41 Rao P, Kadesch T. The intracellular form of notch blocks transforming growth factor β-mediated growth arrest in Mv1Lu epithelial cells. *Mol Cell Biol* 2003; **23**: 6694–701.

42 Takizawa T, Ochiai W, Nakashima K, Taga T. Enhanced gene activation by Notch and BMP signaling cross-talk. *Nucl Acids Res* 2003; **31**: 5723–31.
43 Itoh F, Itoh S, Goumans MJ, Valdimarsdottir G, Iso T, Dotto GP, Hamamori Y, Kedes L, Kato M, ten Dijke P. Synergy and antagonism between Notch and BMP receptor signaling pathways in endothelial cells. *EMBO J* 2004; **23**: 541–51.
44 Blokzijl A, Dahlqvist C, Reissmann E, Falk A, Moliner A, Lendahl U, Ibanez CF. Cross-talk between the Notch and TGF-β signaling pathways mediated by interaction of the Notch intracellular domain with Smad3. *J Cell Biol* 2003; **163**: 723–8.
45 Zavadil J, Cermak L, Soto-Nieves N, Bottinger EP. Integration of TGF-β/Smad and Jagged1/Notch signalling in epithelial-to-mesenchymal transition. *EMBO J* 2004; **23**: 1155–65.
46 Kamei Y, Xu L, Heinzel T, Torchia J, Kurokawa R, Gloss B, Lin SC, Heyman RA, Rose DW, Glass CK, Rosenfeld MG. A CBP integrator complex mediates transcriptional activation and AP-1 inhibition by nuclear receptors. *Cell* 1996; **85**: 403–14.
47 Lee CW, Sorensen TS, Shikama N, La Thang NB. Functional interplay between p53 and E2F through co-activator p300. *Oncogene* 1998; **16**: 2695–710.
48 Webster GA, Perkins ND. Transcriptional cross talk between NF-κB and p53. *Mol Cell Biol* 1999; **19**: 3485–95.
49 Sheppard KA, Phelps KM, Williams AJ, Thanos D, Glass CK, Rosenfeld MG, Gerritsen ME, Collins T. Nuclear integration of glucocorticoid receptor and nuclear factor-κB signaling by CREB-binding protein and steroid receptor coactivator-1. *J Biol Chem* 1998; **273**: 29 291–4.
50 Horvai AE, Xu L, Korzus E, Brard G, Kalafus D, Mullen TM, Rose DW, Rosenfeld MG, Glass CK. Nuclear integration of JAK/STAT and Ras/AP-1 signaling by CBP and p300. *Proc Natl Acad Sci USA* 1997; **94**: 1074–9.
51 Lubman OY, Korolev SV, Kopan R. Anchoring notch genetics and biochemistry: structural analysis of the ankyrin domain sheds light on existing data. *Mol Cell* 2004; **13**: 619–26.
52 Goodman RH, Smolik S. CBP/p300 in cell growth, transformation, and development. *Genes Dev* 2000; **14**: 1553–77.
53 Kopan R, Ilagan MX. γ-Secretase: proteasome of the membrane? *Nature Rev Mol Cell Biol* 2004; **5**: 499–504.
54 Shawber C, Nofziger D, Hsieh JJ-D, Lindsell C, Bogler O, Hayward D, Weinmaster G. Notch signaling inhibits muscle cell differentiation through a CBF1-independent pathway. *Development* 1996; **122**: 3765–73.
55 Muraoka M, Konishi M, Kikuchi-Yanoshita R, Tanaka K, Shitara N, Chong JM, Iwama T, Miyaki M. p300 gene alterations in colorectal and gastric carcinomas. *Oncogene* 1996; **12**: 1565–9.
56 Gayther SA, Batley SJ, Linger L, Bannister A, Thorpe K, Chin SF, Daigo Y, Russell P, Wilson A, Sowter HM, Delhanty JDA, Ponder BAJ, Kouzarides T, Caldas C. Mutations truncating the EP300 acetylase in human cancers. *Nat Genet* 2000; **24**: 300–3.
57 Suganuma T, Kawabata M, Ohshima T, Ikeda M. Growth suppression of human carcinoma cells by reintroduction of the p300 coactivator. *Proc Natl Acad Sci USA* 2002; **99**: 13 073–8.

 doi: 10.1111/j.1349-7006.2005.00048.x

ELSEVIER

EXPERIMENTAL HEMATOLOGY

Experimental Hematology 33 (2005) 1459–1469

Hematopoietic stem cells expanded by fibroblast growth factor-1 are excellent targets for retrovirus-mediated gene delivery

Aleksandra Crcareva[a,b,d], Toshiki Saito[a], Atsushi Kunisato[a,b,e], Keiki Kumano[a,b], Takahiro Suzuki[a,c], Mamiko Sakata-Yanagimoto[a,b], Masahito Kawazu[a], Aleksandar Stojanovic[d], Mineo Kurokawa[a], Seishi Ogawa[a,c], Hisamaru Hirai[a,b], and Shigeru Chiba[a,b]

[a]*Departments of Hematology/Oncology;* [b]*Cell Therapy/Transplantation Medicine, and* [c]*Regeneration Medicine for Hematopoiesis, University of Tokyo, Tokyo, Japan;* [d]*Department of Hematology, Clinical Center, Skopje, Macedonia; and* [e]*Kirin Brewery Co., LTD Pharmaceutical Research Laboratories, Takasaki, Japan*

(Received 6 May 2005; revised 31 August 2005; accepted 1 September 2005)

Objective. **For the study of the function of genes of interest in hematopoietic stem cells (HSCs) and for successful gene therapy, it is fundamental to develop a method of efficient gene transfer into HSCs. In mice experiments, efforts have been made to raise the transduction efficiency by modifying the vectors, administrating 5-fluorouracil (5-FU) to donor mice, selecting cytokine cocktails to better sustain the long-term repopulating potential of the stem cells, and so on. The objective of this study is to examine whether the use of fibroblast growth factor-1 (FGF-1)-expanded bone marrow cells provide an improved source for retroviral gene delivery to HSCs.**

Materials and Methods. **Unfractionated bone marrow cells from one mouse were cultured in serum-free medium containing FGF-1. Both floating and attached cells were transferred to retronectin precoated dishes and infected with virus supernatant from MP34 cells stably transduced with pMY/GFP retrovirus. After 3-day infection, the green fluorescence protein–positive fraction was sorted and the cells were transplanted to lethally irradiated mice.**

Results. **The experiments illustrated that the number of bone marrow–derived competitive repopulation units (CRUs) was increased from 600 to 9300 per mouse after a 3-week culture period with FGF-1. Following retroviral transduction of the expanded cells, the absolute number of sorted retrovirus-transduced CRUs was 4200. Using these retrovirus-transduced cells in noncompetitive reconstitution assay, we achieved radiation protection and long-term bone marrow reconstitution in 100% of the recipients with average myeloid and lymphoid chimerisms of 70% and 50%, respectively, even if we transplanted 150 recipients with cells derived from a single donor mouse.**

Conclusion. **In conclusion, FGF-1-expanded bone marrow cells constitute an excellent source of stem cells that could be used in a range of gene delivery protocols.** © **2005 International Society for Experimental Hematology. Published by Elsevier Inc.**

Hematopoietic stem cells (HSCs) are clonogenic cells with capacity to self-renew and differentiate into progenitor cells and mature blood cells of all hematopoietic lineages. Gene delivery to HSCs is key to the study of genes of interest in HSCs and their various progenies for experimental purposes, as well as for gene therapy of hematopoietic and immune disorders. In most of the experimental protocols for HSC-targeted gene delivery, retrovirus-mediated gene transfer methods have been used. The difficulty is that cell division is requisite for the retrovirus to be introduced into the cells and HSCs are quiescent in nature. The use of lentiviral vectors is more efficient as they do not require cell division for gene transduction, but it requires higher biosafety levels.

Offprint requests to: Shigeru Chiba, M.D., Ph.D., Department of Cell Therapy and Transplantation Medicine, University of Tokyo Hospital, 7-3-1 Hongo, Bunkyo-ku, Tokyo 113-8655, Japan; E-mail: schiba-tky@umin.ac.jp

The present address for Aleksandra Crcareva is Department of Stem Cell Biology, University of Groningen; the present address for Toshiki Saito is Transplantation Biology Research Center, BMT Section, MGH-East, Boston, Massachusetts, USA.

0301-472X/05 $–see front matter.
doi: 10.1016/j.exphem.2005.09.001

It has been a major challenge for the development of HSC culture procedures to allow transplantable stem cells to proliferate without loss of their stem cell activity. Modifications of cytokine combinations used for HSC expansion [1–3] have resulted only in modest improvements in gene transfer into HSCs because any cytokine combination induces some degree of differentiation in the HSCs concomitant with their cell division. As an alternative gene transfer strategy, administration of 5-fluorouracil (5-FU) to donor mice has been used to enrich the HSCs. 5-FU is selectively cytotoxic for cycling cells while forcing quiescent HSCs to go into cycle. It is known that 5-FU administration enhances gene transfer into HSCs up to 10-fold [4] but there is also evidence that treatment with 5-FU reduces the engraftment potential of bone marrow (BM) cells [5].

Recently, a cogent method for in vitro expansion of mouse long-term repopulating cells using fibroblast growth factor-1 (FGF-1) as a single exogenous growth factor was described [6]. We confirmed that this method is highly reproducible and that the growing cells after 3 weeks of this culture contain an abundant number of long-term and multilineage repopulating cells. Thus, we expected that these cells would serve as an excellent source for retrovirus-mediated gene delivery.

Interestingly, limiting dilution experiments revealed that there was a 15.3-fold increase in the number of competitive repopulation units (CRUs) cultured with FGF-1 and that 45% of the expanded CRUs could be recovered by sorting as retrovirus-transduced cells.

Materials and methods

Mice

C57BL/6 (B6-Ly5.2) mice were purchased from Narc (Tokyo, Japan). Mice congenic for Ly5 locus (B6-Ly5.1), gifts from H. Nakauchi (Institute of Medical Science, University of Tokyo, Tokyo, Japan), were bred and maintained at Sankyo Labo Service (Tsukuba, Japan). Ly5.1/5.2 mice were obtained from mating pairs of B6-Ly5.1 males and B6-Ly5.2 females and were maintained in the animal facility of the University of Tokyo. Eight- to 10-week old mice were used as recipients. Mice were treated based on the University of Tokyo Animal Experiment Manual.

Cytokines

The Flt3 ligand (FL) was purchased from Genzyme (Boston, MA, USA), and the other cytokines used were generated in Kirin Brewery Research Laboratory (Takasaki, Japan).

Establishment of virus producing stable cell lines

GP-293 packaging cells (Clontech, Palo Alto, CA, USA) were transiently transfected with vesicular stomatitis virus glycoprotein (pVSV-G; Clontech) and pMY/IRES-EGFP [7] (a gift from T. Kitamura, IMSUT, Tokyo, Japan). After 48 hours, virus supernatant was collected and used to infect ψMP34 cells [8] (a gift from Wakunaga Pharmaceuticals, Hiroshima, Japan), which carries an envelope protein from Molony murine leukemia virus [9,10].

ψMP34 cells expressing green fluorescence protein (GFP) at high levels were clone-sorted with FACS Vantage (Becton Dickinson, Franklin Lakes, NJ, USA) and the clones producing individual viruses at the highest titers were selected.

Virus-producing ψMP34 cells were cultured in 3 mL Dulbecco's modified essential medium (Invitrogen, Grand Island, NY, USA) supplemented with 10% fetal calf serum and penicillin streptokinase in collagen type I–coated plates (Corning Inc., Corning, NY, USA). After 48 hours, when 90% confluence was reached, the culture medium was collected and filtrated through 0.45-μm filters (Pall Corporation, Ann Harbor, MI, USA). Virus was concentrated by centrifugation at 18,000*g* for 4 hours at 4°C. The titer of the concentrated virus was defined by transduction of NIH3T3 cells and analysis of GFP expression with FACS Calibur (Becton Dickinson). All the concentrated viral supernatants showed efficiencies of 3.5 to 4 × 10^8 NIH3T3 cell infection per milliliter.

Stem cell expansion

BM cells were cultured with FGF-1 and heparin as previously described [6]. Briefly, unfractionated BM cells with neither erythrocyte lysis nor gradient centrifugation from a 10- to 12-week-old B6-Ly5.1 mouse were cultured for 3 weeks in 5 mL StemSpan serum-free medium (StemCell Technologies, Vancouver, BC, Canada) in the presence of 10 ng/mL FGF-1 (Invitrogen) and 10 μg/mL heparin (Sigma, St. Louis, MO, USA) in a six-well noncoated plate. The density of the cells was 5 × 10^6 cells/well. Two plates (12 wells) were used to culture BM cells obtained from a single mouse. Twice a week, the medium was changed by removing half the media from the well and gently adding equal amount of the same fresh media without resuspending the cells.

Stem cell enrichment

BM mononuclear cells were obtained from 10- to 12-week-old mice and lineage marker–negative, c-Kit$^+$ and Sca1$^+$ (KSL) cells were sorted with FACS Vantage as previously described [11,12].

Retrovirus gene transfer

A schematic diagram of the transduction protocol of the FGF-1-expanded cells is given in Figure 1B. Six wells from a 24-well noncoated plate were covered with 500 μL of 25 μg/mL RetroNectin (Takara, Shiga, Japan) and incubated overnight at 4°C or 2 hours at room temperature. The wells were then washed with phosphate-buffered saline (PBS) and covered with 2% bovine serum albumin for 30 minutes at room temperature. After being washed with PBS again, 500 μL of the unconcentrated virus-containing medium was put in the wells and incubated at 37°C for 4 hours. Next, the supernatant was discarded and the wells were gently washed with PBS.

After centrifugation of virus-containing medium, the supernatants were removed and the pellets were resuspended in 300 μL of StemSpan medium containing one of the following three cytokine cocktails: 10 ng/mL FGF-1+100 ng/mL stem cell factor (SCF)+100 ng/mL TPO, 100 ng/mL SCF + 100 ng/mL TPO, or 10 ng/mL FGF-1 alone. Then, these concentrated viruses were mixed with a 200-μL suspension of 3.5 × 10^5 cultured cells resuspended in 300 μl of the same cytokine cocktails described above (multiplicity of infection [MOI], 300–340; see below for details).

Subsequently, the 3-week cultured BM cells were collected from one well. The floating and adherent cells were collected by